

Review

# Estimation of Lithium-Ion Batteries State-Condition in Electric Vehicle Applications: Issues and State of the Art

Khaled Laadjal \*  and Antonio J. Marques Cardoso \* 

CISE—Electromechatronic Systems Research Centre, University of Beira Interior, Calçada Fonte do Lameiro, P-62001-001 Covilhã, Portugal

\* Correspondence: laadjal.khaled1991@gmail.com (K.L.); ajmcardoso@ieee.org (A.J.M.C.)

**Abstract:** Lithium-ion batteries are the most used these days for charging electric vehicles (EV). It is important to study the aging of batteries because the deterioration of their characteristics largely determines the cost, efficiency, and environmental impact of electric vehicles, especially full-electric ones. The estimation of batteries' state-condition is also very important for improving energy efficiency, lengthening the life cycle, minimizing costs and ensuring safe implementation of batteries in electric vehicles. However, batteries with large temporal variables and non-linear characteristics are often affected by random factors affecting the equivalent internal resistance (EIR), battery state of charge (SoC), and state of health (SoH) in EV applications. The estimation of batteries' parameters is a complex process, due to its dependence on various factors such as batteries age and ambient temperature, among others. A good estimate of SoC and internal resistance leads to long battery life and disaster prevention in the event of a battery failure. The classification of estimation methodologies for internal parameters and the charging status of batteries will be very helpful in choosing the appropriate method for the development of a reliable and secure battery management system (BMS) and an energy management strategy for electric vehicles.

**Keywords:** lithium-ion battery; electric vehicle (EV); battery management system (BMS); state of charge (SoC); state of health (SoH); equivalent internal resistance (EIR)



check for updates

**Citation:** Laadjal, K.; Cardoso, A.J.M.

Estimation of Lithium-Ion Batteries State-Condition in Electric Vehicle Applications: Issues and State of the Art. *Electronics* **2021**, *10*, 1588.

<https://doi.org/10.3390/electronics10131588>

Academic Editor: Gabriele Grandi

Received: 31 May 2021

Accepted: 27 June 2021

Published: 30 June 2021

**Publisher's Note:** MDPI stays neutral with regard to jurisdictional claims in published maps and institutional affiliations.



**Copyright:** © 2021 by the authors. Licensee MDPI, Basel, Switzerland. This article is an open access article distributed under the terms and conditions of the Creative Commons Attribution (CC BY) license (<https://creativecommons.org/licenses/by/4.0/>).

## 1. Introduction

Energy storage systems (ESS) play a significant role in a wide variety of technical and industrial applications [1,2], either as a mass store of energy or as a dispersed temporary power source. Broad capacity, sufficient strength, lifespan, durability, and protection are among the key parameters considered for energy storage [3]. In response to changing energy requirements and technological advances, the energy storage industry has evolved, adapted and innovated over the past century to be used in both real-time and non-real-time applications [1–5]. This has become of paramount importance in three different areas:

- Production and distribution of electric energy (stationary application);
- Portable tools and devices (on-board application);
- Electric vehicles (EVs).

Compared with other widely used electrical batteries in energy storage applications, lithium-ion batteries are characterized by high energy capacity, high power density, lifetime and environmental friendliness, and thus have seen broad use in the area of consumer electronics [2]. However, automotive lithium-ion batteries (LiBs) have a high capacity and large serial-parallel numbers which, when combined with issues like reliability, durability, uniformity, and cost, puts a constraint on their widespread use in electric vehicle (EV) applications [2,3]. Several EV high-energy battery incidents have lately been recorded. The mishaps have also been blamed for poor fire safety safeguards in BMS. Other factors might add to the dangers of EV batteries. This study explores the scope and significance of different available standards/guidelines that must be investigated in order to develop

BMS standards [4]. The size of the energy storage system in EVs increases with the rate of electrification of vehicles: from stop and start applications in the vehicle, through hybrids and plug-in hybrids, to the 100% electric vehicle. Electric vehicles (EVs) can be narrowly categorized per the power source as follows: solely hybrid electric vehicles (HEVs), battery-powered electric vehicles (BEVs), plug-in hybrid electric vehicles (PHEVs), photovoltaic electric vehicles (PEVs) and fuel cell vehicles (FCVs) [1,2]. The basic battery-powered electrical vehicle system is shown in Figure 1a which comprises a differential, mechanical transmission system, electric motor, power converter (Controller), battery management system (BMS) (Figure 1b), and battery packs [3–7].

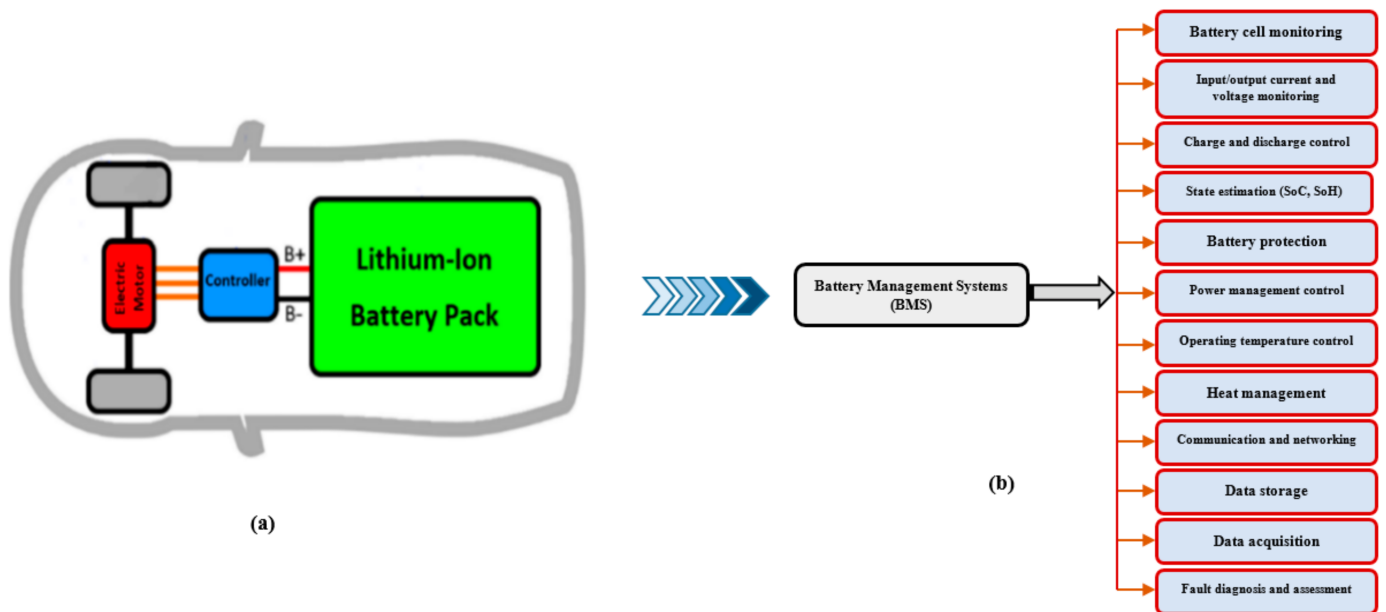


Figure 1. (a) Schematization of the population systems of an EV. (b) Overview of a BMS.

Battery status must still include state-of-charge (SoC) [7] or State-of-Energy (SoE) [8–10], State-of-Health (SoH) [11], and State-of-Power (SoP) [12–14]. The most significant characteristics of SOC estimation techniques for LiBs in EVs are estimate accuracy and computational complexity. Every attempt is made for the different online SOC estimate techniques to enhance the accuracy of the estimation as reliably as is feasible within the restricted on-chip resources. The good estimation of the lithium-ion batteries (LiB) SoC in EVs has many advantages (Figure 2).

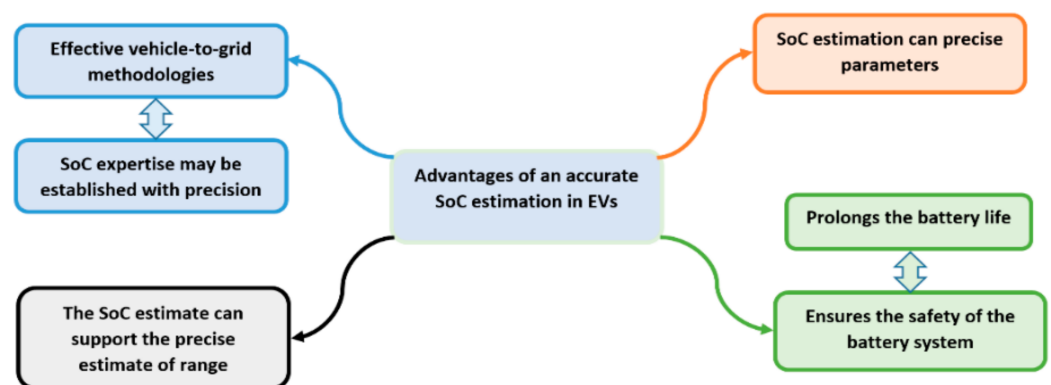


Figure 2. Advantages of an accurate SoC estimation in EVs.

Seminal work has been developed examining the coupled SoC and model parameterization using the Kalman Filter (KF). Possibly the best-known methods involve the Kalman

Filter (KF) [15], Extended Kalman Filter (EKF) [16], Unscented Kalman Filter (UKF) [7], Fading Kalman Filter algorithm (FKF) [17], Strong Tracking Cubature Extended Kalman Filter (STCEKF) [18], Multirate Strong Tracking Extended Kalman Filter (MRSTEKF) [19], Lazy Extended Kalman Filter (LEKF) [20], Particle Filter (PF) [21], Sliding Mode Observer (SMO) [22–27], H-infinity Observer [28–31], and Luenberger observer [32]. For example, a double-observer design SoC and capacity-based estimation is developed using a reduced-order electrochemical model for a composite electrode battery coupled to KF [33]. Moura et al. [34] carried out a hybrid SoC/SoH calculation based on a single-particle model (SPM) and the concept of a back-stepping state estimator for non-linear differential equations. Machine learning techniques for estimating SoH have attracted significant interest in recent years. For example, the support vector machine is widely used as a SoH estimation regression tool [35,36]. For a single LiB cell, Xia et al. [37] proposed experimental research and rule-based failure evaluation of an external short-circuit (ESC) fault, and Chiu et al. [38] developed an electrochemical LiB model that was used to simulate nail penetration and thermal leakage caused by penetration.

A review of the techniques and technologies used for SoC estimation is addressed in [39] where a new classification of established SoC estimation techniques is presented. It is indicated in [39] that the SoC estimation method based on explicitly evaluated process parameters does not really take into consideration sensor noise and closed-loop processing methods, like the Kalman Filter (KF) as well as the controller, are identified as worthy prospects, but the major difficulty of these approaches is the detection of the parameters. Finally, it is recommended that Machine Learning strategies have a perfect SoC model [14]. Li et al. [40] The Luenberger Observer, Sigma Point Kalman Filter (SPKF), and EKF were compared to the SoC estimate. In addition, the sliding-mode Observer (SMO) was added for the SoC estimation comparison. The efficiency of the device was addressed throughout terms of precision, temperature instability, estimate of reliability and sensor loss.

Two measurements are required for an open-circuit voltage (OCV) based SoC estimation: a reliable SoC-OCV curve and the obtaining of a precise OCV. Whereas the SoC-OCV curve for LiBs is relatively constant, it varies with lifespan [41] and temperature [11,13]. Indeed, Equivalent Circuit Models (ECMs) have also been suggested for control-oriented strategies, for estimating the electrical reaction and the rate of heat generation. ECMs are often used for modelling cells because of their flexibility, the way that their variables can be easily obtained, and also because of its ability to adapt in real time [42,43]. Different ECMs are already widely seen in EV, including the Rint [44] and the Thevenin model [32,45]. Filter algorithms are also used to predict the battery state, depending on an equivalent circuit model of defined model parameters. Consequently, temperature, C-rate, SoC and battery aging process often affect the equivalent circuit model parameters. Artificial Intelligence (AI) based learning techniques, such as the modelling of the artificial neural network (ANN), and the support vector machine (SVM), have been suggested [46], which can be very precise depending on the training data.

This paper focuses on the SoC Battery and Internal Equivalent Resistance Estimate and its challenges and issues by studying different existing estimation techniques. The lithium-ion battery characteristics of the EVs are reviewed at the beginning of the article. Following this, the modelling of the lithium-ion batteries with different equivalent circuits is presented. This is followed by an in-depth analysis of the common key technologies of battery state estimation. The various SoC, EIR issues, and challenges are also discussed. In addition, the analysis reflects several considerations and difficulties and offers possible recommendations for the implementation of SoC and EIR estimation approaches for EV applications, which are extremely crucial for the possible creation of novel BMS or even the enhancement of the EV battery management system.

### *The Lithium-Ion Battery Characteristics*

The lithium-ion battery is now an ideal option for electric vehicles' (Table 1) relatively high energy density, low self-discharge rate, high voltage, long service life, high reliability

and rapid charging characteristics [47,48]. Figure 3a compares the different battery energy storage systems (BESS) where LiB is influential in terms of specific energy (Wh/kg) and specific power (W/kg). Li-ion batteries comprise of 2 electrodes, an anode and a cathode, which are separated by an electrolyte. During the charging, the lithium ions travel from the cathode to the anode where they recede during discharge, as shown in Figure 3c. Li-ion batteries use a compound lithium electrode material, compared to non-rechargeable lithium-containing metallic batteries [49–51]. In addition, they are available in wide shapes and sizes, making them suitable for various gadgets other than electric vehicles.

**Table 1.** Advantages and disadvantages of Li-ion batteries compared to other rechargeable batteries [50,52].

Lithium-Ion Battery	
Advantages	Disadvantages
Has a high energy density	Involves the risk of bursting
The rate of charge loss is low	Costly, compared to other batteries
Has a greater number of charge and discharge cycles	Complete discharge damages the battery
Need not be discharged completely	Extremely sensitive to high temperature (degrades very quickly if exposed to heat)
Operates at high voltage	Short lifespan

Most of the metals used in the lithium oxides of the cathode are manganese, nickel and cobalt [52]. Lithium iron phosphate (LiFePo<sub>4</sub>) and lithium sulfide are added to this list. Each of these elements has slightly different electrochemical properties which can be combined according to a recipe specific to each manufacturer. Figure 3b compares the qualitative characteristics of different cathode chemistries.

It includes Lithium-Nickel-Cobalt-Aluminum (NCA), which has an excellent lifespan but involves security issues; and Lithium-Nickel-Manganese-Cobalt (NMC), which performs well in all aspects, in addition to having an excellent energy density. However, manganese-containing cathodes are more sensitive to variations in charge and temperature than other chemistries [53]. Lithium-Iron-Phosphate (LFP or LiFePo<sub>4</sub>) can also be found, which is appreciated for its good lifespan and stability but whose energy density remains low, as well as Lithium Manganese with Spinel structure (LMO), and Lithium-Titanate (LTO). NMC chemistry is selected for its good performance and reliability [54]. Table 2 compares the different commercial lithium-ion batteries [55]. Lithium ion batteries have a high energy density, a high power density, a long cycle life, good environmental adaptability, and a high cell voltage when compared to other materials. However, there are many different types of lithium ion batteries, each with its own set of advantages, such as: LCO, which has a high specific energy; LMO, which has a high specific power; NCA and NMC, which are the cheapest and most thermally stable lithium ion batteries; LFP, which has a flat OCV curve but a low capacity and a high self-discharging rate; and LTO, which has a long lifespan and is quick charging but has low specific energy and a greater cost [45].

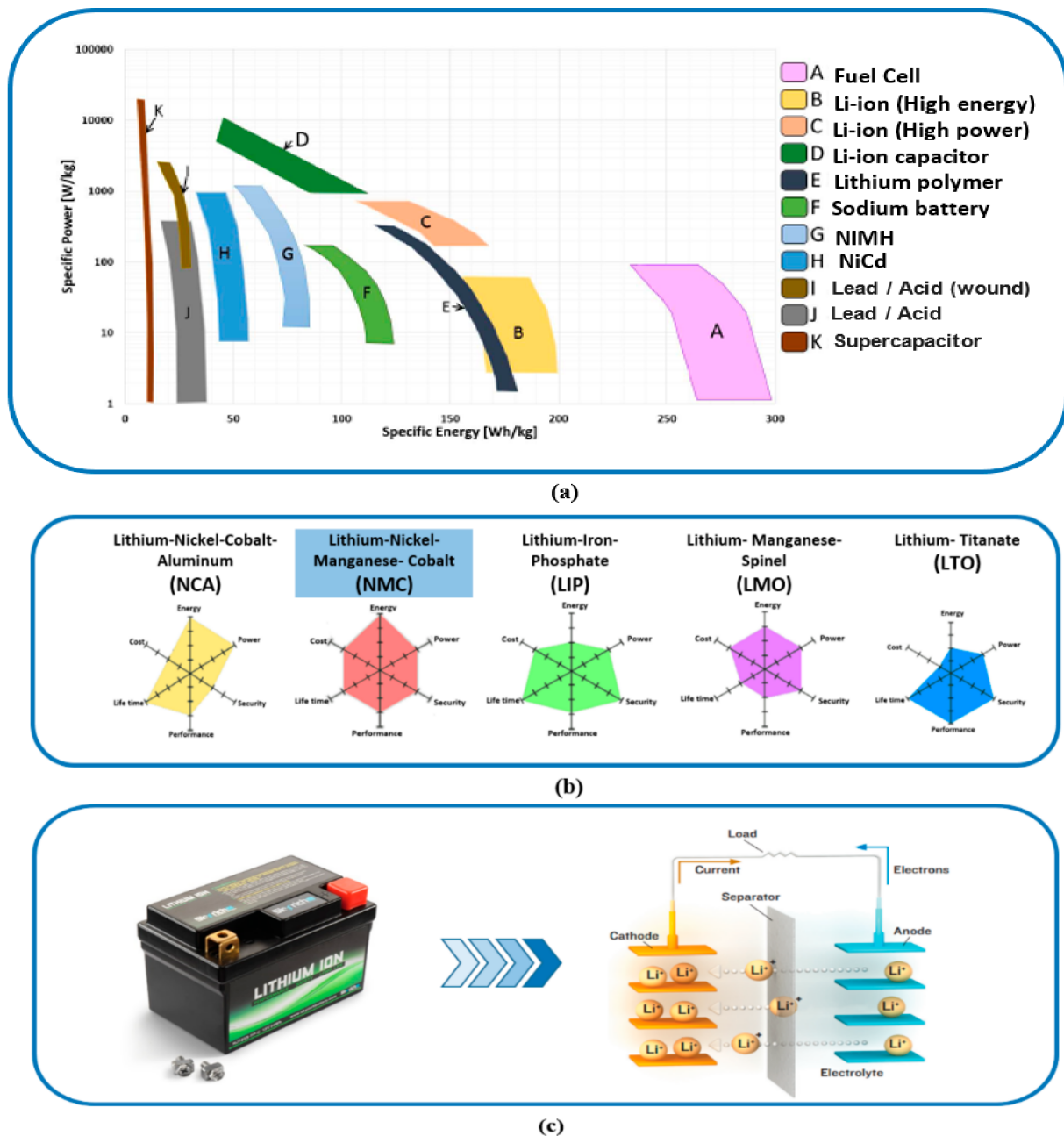


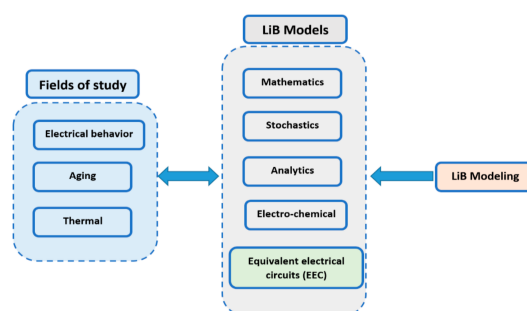
Figure 3. (a) Comparison of power and energy density of different energy storage technologies. (b) Comparison of different lithium chemistries. (c) The transport mechanism of Lithium ions.

Table 2. Comparison of different commercial Lithium-Ion batteries [56].

Battery Name	Abbrev.	Year	Nominal Voltage (V)	Specific Energy (Wh/Kg)	Charge (C)	Discharge (C)	Lifespan	Thermal Runaway (°C)
Lithium cobalt oxide	LCO	Since 1991	3.7–3.9	150–200	0.7–1	1	500–1000	150
Lithium nickel oxide	LNO	Since 1996	3.6–3.7	150–200	0.7–1	1	>300	150
Lithium manganese oxide	LMO	Since 1996	3.7–4.0	100–150	0.7–1	1	300–700	250
Lithium nickel manganese cobalt oxide	NMC	Since 2008	3.8–4.0	150–220	0.7–1	1	1000–2000	210
Lithium iron phosphate	LFP	Since 1993	3.2–3.3	90–130	1	1	1000–2000	270
Lithium nickel cobalt aluminum oxide	NCA	Since 1999	3.6–3.65	200–260	0.7	1	500	150
Lithium titanate	LTO	Since 2008	2.3–2.5	70–85	1	10	3000–7000	.

## 2. Modelling of LiBs

A review of the different battery modelling methods is presented in [57]. A model can be coarse or fine, depending on the level of detail of the problem to be solved. For example, to model the effect of the number and location of the electrodes connecting the electrodes to the poles of cylindrical cells on the distribution of current and temperature, a high resolution electrical, thermal and electrochemical model was developed in [58]. The problem of battery modelling was first tackled by chemists [59,60]. Thus, several studies carried out in this field of study are based on equations drawn from the thermodynamic study of chemical reactions in a cell [61]. Several families of models have been developed, each one meeting specific needs. The families of models are illustrated in Figure 4.



**Figure 4.** Families of models and fields of study of LiBs.

### 2.1. Electrochemical Modelling of LiBs

Electrochemical modelling, unlike equivalent circuit modelling methods, directly reflects the chemical processes that occur in the battery. These models are the most precise battery models because they illustrate the battery processes in great detail. However, the detailed explanation adds to the numerical complexity, and simulating a charge/discharge period with a detailed battery model will take hours if no model reduction technique is used to handle the battery equations. Developing electrochemical battery models can be done in several ways. A lumped parameter model, in which the battery is represented by a small collection of differential algebraic equations (DAEs) that represent the time-dependent electrochemical phenomena between the electrodes, while assuming a uniform spatial distribution of chemical properties, is one of the most common approaches [58]. The bulk of the early physics-based battery models uses this approach, which is often used to describe basic lead-acid and non-rechargeable batteries [54,59]. The key disadvantage of the lumped parameter method is that simple DAEs are inadequate to explain the complicated electrochemical processes in most modern batteries, such as Li-ion cells manufactured using today's advanced technologies [32–35,62].

Rapid advancements in battery science, which have resulted in new electrode materials and battery architectures, necessitate the development of improved models that can explain more nuanced electrochemical and physicochemical processes. The invention of porous electrode theory to characterize models for Li-ion cells was pioneered by Newman et al. [61]. Today, this approach serves as the basis and norm for most physics-based battery modelling techniques and it is often used to generate battery testing data for model validation. This model depicts a battery in great detail, considering all significant chemical performance such as mass transfer and diffusion, ion distribution, side reactions, temperature effects, and battery aging. The porous electrode and condensed solution theories, which explain charge, discharge, and species transport in the solid and electrolyte phases across a generalized one-dimensional spatial cell structure, are the basis for the majority of current rigorous battery models. In comparison to lumped-parameter modelling, the porous electrode theory describes electrochemical processes using partial differential equations (PDEs). Fick's law of diffusion for active material concentration, Ohm's law for electrical potential distributions, and the Nernst and Butler-Volmer equations are used to derive these PDEs in general (Figure 5).

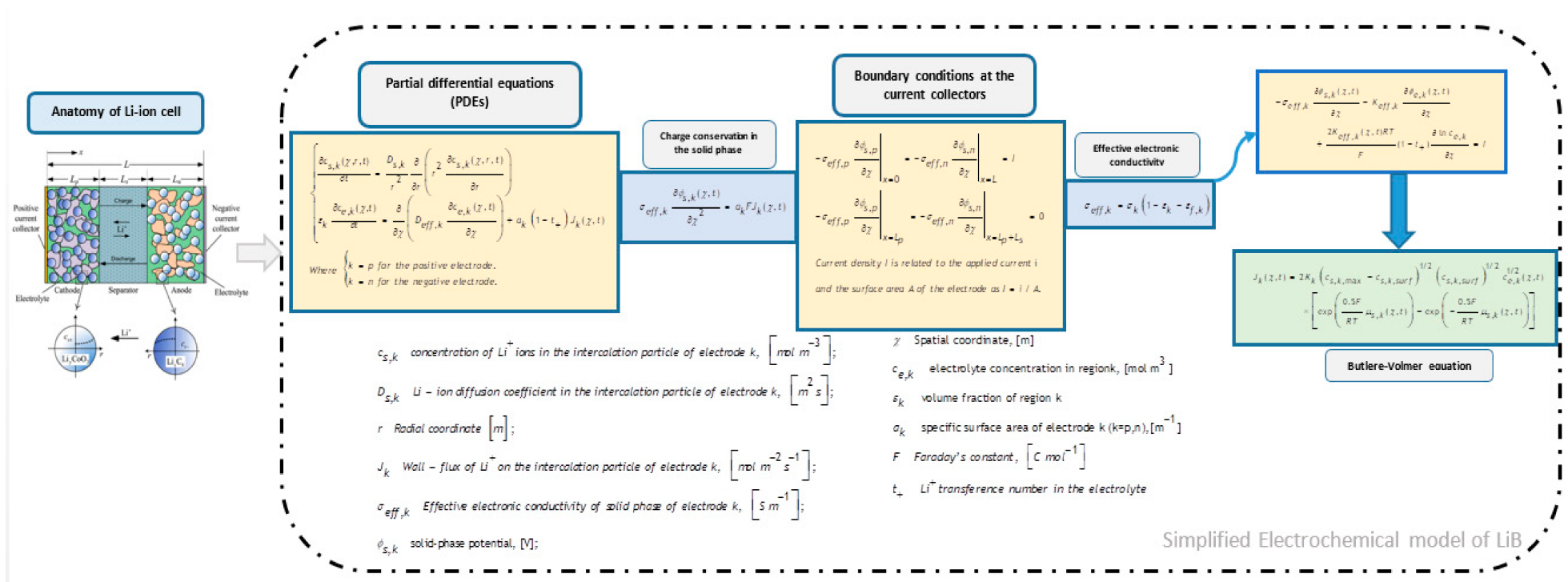


Figure 5. Electrochemical model of LiB.

## 2.2. Equivalent Circuit Models for LiBs

Equivalent Circuit Models (ECMs) for Lithium-ion Battery cells are being used to evaluate the state of the battery in order to explain the current-voltage properties of the battery. ECMs can be constructed for various aims, such as accuracy, parameterization of computational load and efficiency, where model parameters can be tested through experimentation and optimization techniques. Due to the technology, type and application of the battery, there is no definitive answer to the choice of the most appropriate ECM. Different studies are recommending different models [54,63]. The effect of the optimization approach on the computational load was only regarded by Lai et al. [63]. This indicates that the findings and guidelines of different statistical load studies are not strictly equivalent if various evaluation approaches are used. However, due to the implementation and the exchange of accuracy, reliability and performance, basic models are usually favored. The 1RC [64,65], and 2RC [66–68] are commonly used ECMs [69].

SoC evaluation based on an ECM model requires the derivation of circuit models composed of various circuit elements constructed in series or parallel combinations in order to reproduce the dynamics of the battery. The various ECM schemes have been suggested in Table 3. The Thevenin model [55,70] is used as a standard ECM which is designed using a single RC group, resistance, and voltage source, as shown in Table 3 [71,72]. The DP and Thevenin models exhibit stronger dynamic properties, indicating that these two models are more suited for simulating lithium-ion batteries. In [54], it is demonstrated that the Rint model cannot accurately represent the dynamic performance of the power battery since the polarization characteristic has been disregarded. Both the PNGV and Thevenin models can replicate polarization properties. The PNGV model differs from the Thevenin model in that it includes an extra capacitor to account for the impact of the open circuit voltage. However, it will create a fluctuation in the battery model, resulting in a significant error. The terminal voltage predicted using the Thevenin model shows higher dynamic performance when compared to the experimental data, with a maximum error rate of less than 1%. The RC model's large inaccuracy also shows that it requires significant development and optimization. When compared to other models, the DP model can mimic the battery with superior dynamic characteristics and the least error, indicating that it is both accurate and reasonable. On the other hand, the suggested DP model has the best dynamic performance and provides a more accurate SoC estimation.

**Table 3.** Lithium-ion battery equivalent circuit models [54].

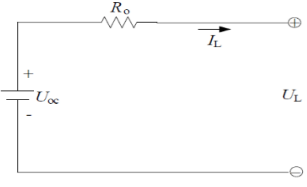
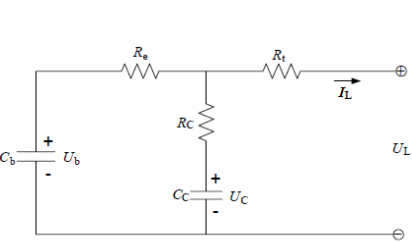
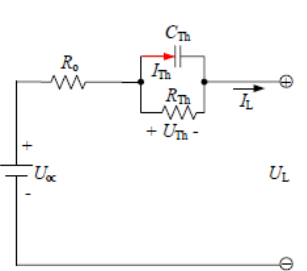
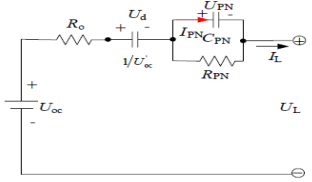
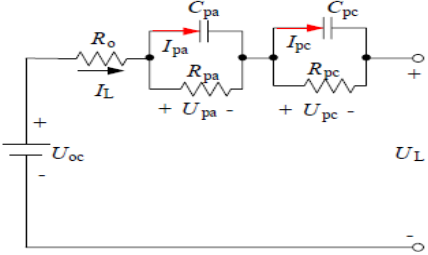
Equivalent Model	Schematic Diagram	Characteristics
<p><b>The Rint model</b></p>		<p><math>R_o</math> and open-circuit voltage <math>U_{oc}</math> are functions of <math>SoC</math>, <math>SoH</math>, and temperature.  <math>I_L</math>: load current  <math>U_L</math>: is the terminal voltage.                      ...  <math>U_L = U_{oc} - I_L R_o</math> (1)</p>
<p><b>The RC model</b></p>		<p><math>C_c</math>: a small capacitance represents the surface effects of a battery, and it is named surface capacitor.  <math>C_b</math>: a very large capacitance represents bulk capacitor.  <math>R_t, R_e, R_c</math>: are terminal resistor, end resistor and capacitor resistor. <math>U_b</math> and <math>U_c</math> are the voltages across <math>C_b</math> and <math>C_c</math>, respectively.  <math display="block">\begin{bmatrix} \ddot{U}_b \\ U_c \end{bmatrix} = \begin{bmatrix} -\frac{1}{C_b(R_e+R_c)} &amp; \frac{1}{C_b(R_e+R_c)} \\ \frac{R_c}{C_c(R_e+R_c)} &amp; -\frac{R_e}{C_c(R_e+R_c)} \end{bmatrix} \begin{bmatrix} U_b \\ U_c \end{bmatrix} + \begin{bmatrix} -\frac{R_c}{C_b(R_e+R_c)} \\ -\frac{R_e}{C_c(R_e+R_c)} \end{bmatrix} [\ddot{I}_L]</math> (2)  <math display="block">[\ddot{U}_L] = \begin{bmatrix} \frac{R_c}{(R_e+R_c)} &amp; \frac{R_e}{(R_e+R_c)} \end{bmatrix} \begin{bmatrix} \ddot{U}_b \\ U_c \end{bmatrix} + \left[ -R_t - \frac{R_e R_c}{(R_e+R_c)} \right] [\ddot{I}_L]</math></p>
<p><b>The Thevenin model</b></p>		<p><math>U_{oc}</math>: Open-circuit voltage,  <math>R_o</math>: Internal resistances and equivalent capacitances.  <math>R_{Th}</math>: The polarization resistance.  <math>C_{Th}</math>: The equivalent capacitance used to describe the transient response during charging and discharging.  <math>U_{Th}</math> is the voltages across <math>C_{Th}</math>.  <math>I_{Th}</math> is the outflow current of <math>C_{Th}</math>.  <math display="block">\begin{cases} \ddot{U}_{Th} = -\frac{U_{Th}}{R_{Th}C_{Th}} + \frac{I_L}{C_{Th}} \\ U_L = U_{oc} - U_{Th} - I_L R_o \end{cases}</math> (3)</p>

Table 3. Cont.

Equivalent Model	Schematic Diagram	Characteristics
<p>The PNGV model</p>		<p>Adding a capacitor <math>1/U_{oc}</math> in series, based on the Thevenin model, to describe the changing of open circuit voltage generated in the time accumulation of load current.</p> $\begin{cases} \ddot{U}_d = U_{oc} I_L \\ U_{PN} = -\frac{U_{PN}}{R_{PN} C_{PN}} + \frac{I_L}{C_{PN}} \\ U_L = U_{oc} - U_d - U_{PN} - I_L R_o \end{cases} \quad (4)$
<p>The DP model</p>		<p><math>U_{oc}</math>: Open-circuit voltage.  <math>R_o</math>: Internal resistances, such as the ohmic resistance.  <math>R_{pa}</math>: The polarization resistances, and electrochemical polarization.  <math>R_{pc}</math>: The effective resistance characterizing concentration polarization.  <math>C_{pa}</math> and <math>C_{pc}</math>: Used to characterize the transient response during transfer of power to/from the battery, and to describe the electrochemical polarization and the concentration polarization separately.</p> $\begin{cases} U_{pa} = -\frac{U_{pa}}{R_{pa} C_{pa}} + \frac{I_L}{C_{pa}} \\ U_{pc} = -\frac{U_{pc}}{R_{pc} C_{pc}} + \frac{I_L}{C_{pc}} \\ U_L = U_{oc} - U_{pa} - U_{pc} - I_L R_o \end{cases} \quad (5)$

### 3. Battery State Estimation Methods

The methods for estimating the status of the battery are being used to characterize the state of the battery bank required to run the battery-powered device efficiently, sustainably and safely, due to the operating environment conditions and the non-linear behavior of electrochemical reactions. Established state variables typically characterize the three characteristics of the battery: the amount of charge stored, the decrease in the maximum capacity compared to the new battery, and the quantity of energy the battery can produce, as most frequently defined by SoC, SoH, SoF, or alternatives. A short basic introduction of the major approaches is already categorized into three groups: experimental methods, model-based methods and data-driven methods.

Experimental methods as described here are procedures, which investigate the properties of the battery by means of non-destructive experimental treatments. Experimental methods are only better suited for offline SoH identification due to experimental necessary conditions, like time duration, constant temperature, and disconnected batteries, even though people have tried to attain online functionality, including the obtained static SoH charging in real-time, ICA partial charging [73] detection, or online EIS for fuel cell EVs [74]. Different techniques are generally used in conjunction with model-based approaches, also including Hybrid Pulse Power Characteristics (HPPC) for the detection of model parameters [75]. The model-based approach relies on the use of an approximate equivalent model to describe the dynamics of the battery, via an adaptive filtering of the available data sensor for estimating non-observant state parameters.

#### 3.1. The SoC Estimation Method

The status of charge explains the quantity of energy stored in the battery [76,77]. SoC is not a physical property which can be directly measured. The only procedure to measure the SoC is to correlate indirectly some amounts, such as voltage, current and temperature [78] and is usually expressed as a percentage of nominal energy (capacity). In the literature, SoC is described as the ratio between both the usable charge (capacity or energy) and the total charge of the battery [79]. The mathematical definition of SoC [72] is expressed in the following:

$$\text{SoC} = \frac{Q_{\text{available}}}{Q_{\text{rated}}} \quad (6)$$

The proper functioning of the EV strongly depends on the functioning of the BMS. A BMS is an electronic system for managing the rechargeable battery by checking the status and parameters of the battery [80]. SoC is one of the core parameters of the battery system, i.e., the amount of charge left in the cell. Good prediction of SoC precision contributes to better battery life and disaster avoidance in the case of a battery failure. In addition, accurate SoC estimation is of greater importance for efficient EV work. Nevertheless, its reliance on different parameters, like the battery age, ambient temperature and many other variables, makes the estimation of SoC a complex process. Based on recent research papers on SoC estimation methods (Table 4), SoC estimation techniques can be classified into five classes [77]: OCV-based estimation, coulomb-counting based estimation methods, model-based estimation methods, machine-based estimation methods, and modern control theory-based estimation, as shown in Figure 6.

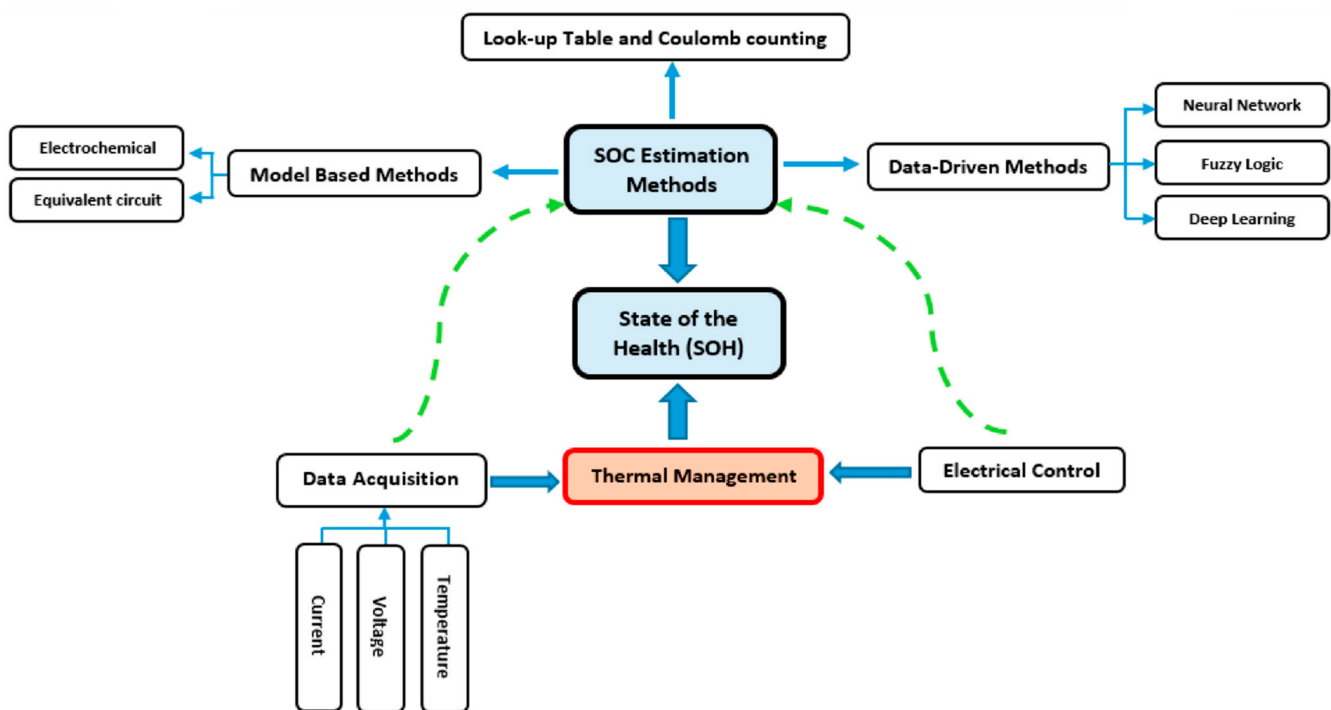


Figure 6. Classification of SoC estimation methods.

Each class needs to adopt various approaches to evaluate the SoC performance. According to the history of SoC battery development, it is expected that as rechargeable batteries become available, so will SoC research [72]. To date, SoC always has been a popular spot and a main research point. Established SoC estimation strategies can also be divided into different categories; the standard method, the adaptive filter method, the learning algorithm, the non-linear observer, and the hybrid algorithm [81,82]. OCV is a methodology that utilizes the electromotive force of the stable battery in the open-circuit state and the SoC ratio to estimate the SoC value [14]. For the relationship between the SoC and OCV, there is an approximate relation, but it is not necessarily the same for all batteries, it depends on the power magazine in the battery and the properties of the materials (electrode).

The impedance and the EIR of the lithium-ion battery can also be used when the temperature, SoC, and SoH are fixed to define the electrical characteristics of each current. Nevertheless, it is very hard to identify and evaluate in real time the electrical impedance spectroscopy (EIS) because the relationship between the SoC and impedance is not stable, and the cost is expensive, due to sinusoidal, alternating current (AC) may also be needed. Even though impedance is achieved, compared to the relation between SoC-OCV, the relationship between impedance and SoC is not stable. The main issues are:

1. The change in impedance is not sensitive to variations in SoC for a certain range of SoCs, and there may be a non-monotonic relationship between impedance and SoCs;
2. The change in impedance is more sensitive to changes in temperature than to the change in SoC [138–144] and, as a result, it is difficult to compensate for the influence of temperature;
3. Impedance changes a great deal with SoH [138,140–142] and therefore recompense for the aging effect must be considered;
4. The impedance may change over time due to historical and current working conditions [138];
5. Online impedance measurement will contain contact impedance;
6. It is difficult to assess the change in the impedance between LiB cells [143].

**Table 4.** Lithium-ion battery state of charge estimation methods.

	Authors	Description	Applications	Advantages	Disadvantages
<b>OCV based estimation</b>	[83–86]	The SoC-OCV curve is reliable and the OCV curve is very accurate. While this SoC-OCV curve is relatively stable for LiB, it modifies with the life cycle.	Lead Acid, Lithium, Za/Br.	<ul style="list-style-type: none"> <li>* Online.</li> <li>* Easy to implement.</li> </ul>	<ul style="list-style-type: none"> <li>* Needs the battery to be in the resting mode for a long time.</li> <li>* Only accurate when the SoC is very high or very low.</li> <li>* Sensitive to temperature.</li> <li>* Low dynamic.</li> </ul>
	[87–89]	A reliable SoC-OCV curve and a precise OCV. But it changes also with life cycle and temperature.			
	[90,91]	The estimate, largely dependent on the OCV, is only used for a sufficiently long rest time in a particular operating condition, i.e., 3 h can be an appropriate rest time for most working conditions.			
	[92,93]	Some empiric models may be used to estimate the OCV or may be combined with a theoretical analysis.			
	[94,95]	Models via an OCV estimate are not very well suited to SoH or changes in temperature.			
	[96]	An adaptive method for estimating OCVs for online applications.			
	[97]	When the LiFePO <sub>4</sub> cathode is used in the LiB. The SoC estimate based on the OCV within the SoC range of the flat SoC-OCV curve is not accurate.			
<b>Ampere-hour counting estimation (AHC)</b>	[98,99]	AHC evaluation has very limited computation costs and hence it is frequently used for online SoC estimation.	All battery systems, most applications.	<ul style="list-style-type: none"> <li>* Easy to implement.</li> <li>* Accurate if:               <ol style="list-style-type: none"> <li>1. enough recalibration points are available.</li> <li>2. Good current measurements.</li> </ol> </li> </ul>	<ul style="list-style-type: none"> <li>* Depends on the initial SOC, needs accurate initial conditions.</li> </ul>
	[100]	For the AHC methods, the precision may be fair, such as daily adjustment of the initial SoC and capacity and modifying the current drifting sensor.			
<b>Equivalent Circuit Model (ECM) based estimation</b>	[101–104]	Estimate SoC directly by identifying the parameters of the ECM.	All battery systems, most applications.	<ul style="list-style-type: none"> <li>* Online.</li> <li>* SoH estimation</li> </ul>	<ul style="list-style-type: none"> <li>* Sensitive to temperature.</li> <li>* Sensitive to frequency.</li> <li>* Sensitive to the measurement noise.</li> </ul>
	[105,106]	The use of an adaptive model will improve the precision of the system, but also increases the sophistication of the model.			
	[107]	The identification in real time of the parameters needs an additional central processing unit (CPU) load and even more storage space.			
	[108–111]	Precision of conventional ECM voltage in the low range of SoCs.			
<b>Electrochemical model based estimation</b>	[112]	Reduced-order on-board thermal electrochemical model (ROTM). On-board ROTM estimates the voltage and SoC of the single cells and the pack level, using a simpler, high-speed module system with greater accuracy than the commonly used ECM.	All battery systems, most applications.	<ul style="list-style-type: none"> <li>* Accurate.</li> <li>* Complete.</li> <li>* All information about battery conditions.</li> </ul>	<ul style="list-style-type: none"> <li>* Difficult to implement.</li> <li>* Expensive methods.</li> <li>* Offline.</li> </ul>
	[113,114]	The calculation of SoC can be made directly by identifying the amount of LiB in the negative or positive electrodes of the electrochemical model.			
	[115–117]	A new SOC is updated by using a predefined SoC to obtain model voltage and used an electrochemical model and to evaluate it to the measured voltage.			

Table 4. Cont.

	Authors	Description	Applications	Advantages	Disadvantages
	[86]	Partial differential equations, for considering secondary reactions, must also be integrated to the electrochemical model, which will again improve the model complexity.			
Machine learning based estimation	[118,119]	Battery state estimates using data learning techniques have been associated with new advancements in artificial intelligence (AI) such as computer vision and autonomous vehicles. E.g. the Adaptive Neuro-Fuzzy Inferential Method (ANFIM).	All battery systems, most applications.	<ul style="list-style-type: none"> <li>* Easy to implement.</li> <li>* Doesn't need model.</li> <li>* Online.</li> </ul>	<ul style="list-style-type: none"> <li>* Accuracy is strongly dependent on the richness of training data.</li> </ul>
	[120,121]	A vast quantity of data is recorded and processed in a partly or entirely automatic manner in order to meet the nature and usage of the battery. This volume of data has made it possible to boost BMS output through Big Data, the Internet of Things (IoT), data storage, and the ML methodologies being analyzed.			
	[122]	Based on ML methodologies, SoC and SoH are estimated. The main computational load required by these techniques happens mostly during offline training process, which enables the implementation of typical BMS hardware.			
	[82,123,124]	Full review of the use of machine learning techniques for estimating SoC, SoH, SoP and other battery states.			
	[122]	It is shown that FNN is suitable for estimating the SoC battery at various temperatures, such as low temperatures like 20 °C.			
	[125]	The internal resistance data obtained from the laboratory tester was used, as well as the voltage, current and temperature of the battery, to form and test the SoC estimation by the FNN.			
	[126]	Introduction of a procedure to methodically modify the FNN structure using offline optimization technique to identify the optimum FNN structure. SoC is estimated using the general structure selected for the calculation of the initial cost (mean square error) to be used in the next step.			
Modern control theory based estimation	[32,126–128]	With an acceptable input gain by comparing the voltage model with the observed, the actual SoC could be changed. The algorithm calculates the gain. Luenberger is one of the easiest observers.	All battery systems, Photovoltaic, Hybrid Electric Vehicles.	<ul style="list-style-type: none"> <li>* Accurate (if the model is accurate).</li> <li>* Online.</li> <li>* Dynamic applications.</li> </ul>	<ul style="list-style-type: none"> <li>* Needs a suitable battery model.</li> <li>* Initial parameters' problem.</li> <li>* Non-linear and not easy to implement.</li> </ul>
	[129,130]	KF family algorithms are a better choice for more appropriate feedback gain.			
	[10,130–132]	EKF is a commonly used and studied SoC estimation algorithm. The main theory of the EKF algorithm is to identify the correct efficiency of the filter by assessing the model and quantifying the noise. However, the literature suggests that EKF may lack robustness and cannot guarantee an optimal feedback gain due to the linearization of non-linear LiB systems.			

Table 4. Cont.

	Authors	Description	Applications	Advantages	Disadvantages
	[95,132–134]	Unscented Kalman Filter (UKF); the calculation complexity is increased.			
	[135–137]	The precision of the SoC estimation, based on modern control systems, is directly associated to the precision of the battery voltage model. Battery voltage model parameters change with aging and LiB temperature. For the KF family, and due to changes in model parameters over the life of the battery, joint or dual KF family algorithms may be used.			
	[136]	Used an update method for an on-board parameter, but not based on a joint or double KF method.			

Generally, the precise estimation of SoC can also be obtained through the electrochemical theoretical model. However, this model is only appropriate for the offline configuration and efficiency study of lithium-ion batteries. Even so, owing to the high difficulties to analyze the electrochemical model, and the great number of parameters of the battery model, this technique becomes too difficult to use for SoC online evaluation [144]. Two technical methods are generally used to estimate SoC by using the equivalent circuit model. The first model is a common way of estimating SoC directly by identifying the ECM parameters. The second approach uses a predetermined SoC to operate the OCV. The relationship between SoC and OCV is very beneficial, not just in estimation of the OCV based estimation but also in the estimation of the model-based estimation, and then evaluates the voltage of the lithium-ion battery via the ECM [14].

### 3.1.1. Model-Based Estimation Method

In order to ensure and improve the precision and the reliability of the SoC battery estimation by minimizing the effect of noise on the model, the new control theory based on an adaptive filtering algorithm offers another tool for estimating SoC. Figure 7 shows the flowchart of the adaptive filter.

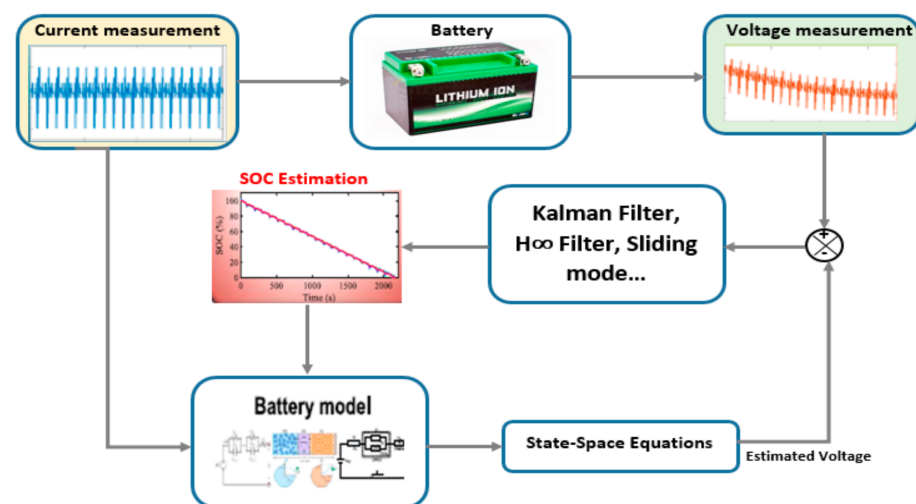


Figure 7. General scheme presenting the adaptive filter algorithm of the SoC estimation techniques.

An algorithm related to modern control theory is developed in [14]. Many non-linear state estimation algorithms and adaptive filters are used to estimate or deduce the internal state of the batteries. Typical algorithms are the Kalman filter [145–147], the Luenberger observer [32], the PI (integration of proportion) observer [148], the H $\infty$  observer [149], and the sliding mode observer [24,86], among others. The Kalman filter is becoming a basic method for non-linear estimation and machine learning applications [150]. In [123,147] an analysis is presented on the different SoC estimation approaches and algorithms. A detailed interpretation, including model advantages, disadvantages, and estimation error, is widely reviewed. The study recognizes that new approaches are simple to adopt but are greatly influenced by aging, environmental disruptions, and especially by temperature. Then, it is noted that an adaptive filter technique will predict a non-linear dynamic state for an acceptable accuracy, lower computational cost, and high performance. However, the approach suffers from high computational pressures and low robustness. The learning technique is also well suited for modelling a non-linear complicated system, considering aging, temperature, and noise.

In [151], the authors suggest a collision warning system that provides the linked automated vehicle and the alert driver when the collision time (TTC) is below defined thresholds. After the remote vehicle BSM preprocessor data, this idea transforms the Remote Vehicle (RV) position and calculates the relative one, distance and speed. The RV

direction is then calculated using the Kalman Filter algorithm and the estimated error for the latitude and longitude estimations are evaluated. Through choosing this approach, the electric vehicle will draw up its surrounding protection radar map and make reasonable decisions, based on the locations of the RV itself and its vicinity, as well as the expected routes. The location and trajectories of surrounding cars is used for the creation of a local driving climate. A novel adaptive technique for the detection of model parameters on different temporal and spatial scales is developed in [103]. Dynamics of the battery are represented in a second-order equivalent circuit model (ECM) incorporating slow dynamics and fast dynamics, independently. The parameter recognition algorithm consists of two distinct units, one for the recognition of the investigated effect, and the other for the identification of fast dynamics. The two components are performed on different time scales. The recursive least square (RLS) is used for the fast dynamics module, and the Extended Kalman Filter (EKF) is used for the slow dynamics' detection module. The relation between the two modules is defined by the voltage response of the slow dynamics. The SoC time scale determination is more adaptive since the time scale of the identification of each module is not fixed, but depends on the current profiles.

In order to ensure timely maintenance and the safety of battery systems, it is important to establish a consistent battery model and precise calculation of battery parameters to characterize the complex behavior of the battery. The contribution in [152] focused on SoC adaptive model estimation of lithium-ion batteries. Therefore, the main idea is composed of three steps. First, a first-order equivalent circuit of the battery model is used to define the functional properties of the battery. The least square recursive method and the off-line detection technique were being used to set high initial values for the model parameters to ensure filter consistency and reduce the convergence rate. Finally, the Extended-Kalman-Filter (EKF) is used for on-line calculation of the SoC battery and model parameters. To improve the efficiency of the EKF process and to modify the model parameters, the first order Taylor approximation of the battery model, which includes inherent model errors, and a proportional integral error modification technique, is used. Accurate state-of-the-charge (SoC) assessment is crucial to the safety and efficiency of BMS in EVs applications. In [110], three common model-based filtering techniques, including Kalman Extended Filter (EKF), Kalman Unscented Filter (UKF), and Particle Filter (PF), are used to estimate SoC and their efficiency in terms of tracking precision, computational time, robustness against instability of initial SoC values, and battery depletion. The comparative results showed that:

- The UKF was more reliable than the EKF and the partial filter when the SoC was properly configured;
- The UKF was more robust to initial values of SoC;
- At the beginning of the SoC calculation, the PF demonstrated a quicker convergence potential than the UKF and the EKF;
- The EKF and the UKF have become more computationally effective than the PF;
- All proposed algorithms were able to estimate the SoC of the aged battery.

The monitoring of the battery system needs a well-designed BMS with a series of current and voltage sensors, necessary to properly monitor the properties of the battery. A safe and stable diagnostic framework must be built in the event of defects in the sensors used. The main idea of the technique proposed in [153] is based mostly on a model-based fault diagnosis scheme for detecting and isolating current and voltage sensor faults, which is implemented in the battery pack series, by using the adaptive extended Kalman Filter.

An online estimation method to estimate the SoC of a lithium iron phosphate (LiFePO<sub>4</sub>) battery is proposed in [17], centered on a simple model, and the OCV of the battery is determined by two cascaded linear phases filter for real-time application. In the first step, a recursive least square filter is used to continuously approximate the parameters of the battery model online and then, from these parameters, a fading Kalman Filter (FKF) is used to estimate the OCV. This technique can avoid the probability of significant calculation errors that could arise with a traditional Kalman Filter due to its ability to compensate for

any modelling error by a fading factor. Compared to the ordinary Kalman Filter, the errors in calculating the SoC battery in urban dynamometer driving schedules-based tests and actual vehicle driving time studies were below 3%.

A novel viewpoint on the error of SoC estimation techniques is suggested in [14]. SoC estimation methods are evaluated from the perspective of calculated values, models, algorithms and state conditions, considering the operation conditions. The probability of more reliable and applicable SoC estimation methods is discussed and the potential development of efficient online SoC estimation methods is suggested. Future developments suggested by the authors, based on the online SoC estimation methods, are also discussed. It is concluded that the OCV estimation should further focus on modelling the aging, temperature, and hysteresis induced SOC errors. The assessment of the SoC and SoH of the battery models, which is characterized and based on physic-high-fidelity, and the control mechanisms are regularly applied to the production of acceptable models that achieve key device characteristics but are computationally accurate. A multi-time approximation for the state calculation of a class of uniquely disrupted structures is proposed in [7]. Assumptions on internal models and complex error prediction mechanisms were specifically stated. Based on these aspects, and on the obtained models, the ability of this estimation system has been shown by both the EKF and the UKF in [108,110], as a core aspect of the online SoC calculation program for lithium-ion batteries. The offline low-current OCV test and the incremental OCV for the predetermination OCV-SoC are widely-used tests by battery makers, BMS designers, and researchers. Two SoC estimators are developed on the basis of two OCV measures. The ambient temperature affects the OCV-SoC relationship, and thus affects the SoC model-based battery estimation. (See Figures 8–14 below) Figure 15 presents a comparative analysis of model-based state estimation methods.

A novel SoC estimation technique is proposed in [154]. The main idea is the SoC value represents mileage longevity and an accurate SoC value is needed to ensure the safe use of the battery to avoid overcharging and over-discharging. However, centered on the Cubature KF and the Particle Filter (PF), a CPF is proposed for precise and effective SoC estimation. The dynamic output of the battery is calculated using the model of the second-order resistor-capacitor (RC) equivalent circuit, and the parameter values were calculated by fitting. The Dynamic Stress Test (DST) was used to approximate the precision and reliability of the CKF and CPF algorithms separately. Usually, the specifications of the battery model vary across the battery life. In [155] it is proposed that a double-scale dual adaptive filter is used to evaluate, in real time, the parameters and SoC estimation of lithium-ion batteries. The Thevenin model was used for the lithium-ion battery modelling. Then, a dual-scale particle filter is introduced and added to the battery parameters and the SoC estimation of Lithium Nickel Manganese Cobalt Oxide (NMC) batteries for different aging conditions. Figure 9 covers the recent literature on the topic of the adaptive filter algorithm for SoC estimation.

### 3.1.2. Data-Driven Based Estimation Methods

Data-driven machine learning approaches to battery state estimation are already powered by huge innovation in artificial intelligence (AI) [118,142] in areas such as machine vision and hybrid vehicles. Figure 10a illustrates how the AI domain is divided with machine learning as well as its corresponding divisions of classification tasks and profound learning [119,156–166]. Figure 10a also demonstrates how the state of the art of SoC and SoH estimation methods for EVs are confined in the field of AI while pervading other sub-areas of machine learning. ANNs have the capability of self-learning and the ability to adapt needed to demonstrate the non-linear model [14]. Without looking at the internal properties and the structure of the battery and the initial SoC information, ANNs could use training data to estimate SoC. Usually at least three layers are being used to create an ANN methodology, consisting entirely of an input layer, one or even more concealed layers, and an output layer. A new SoC estimation technique based on Levenberg-Marquardt (L-M)

Algorithm Configured Multi-Hidden-Layer Neural Network (WNN) Model and a series of novel artificial intelligent-based approaches are developed in [167].

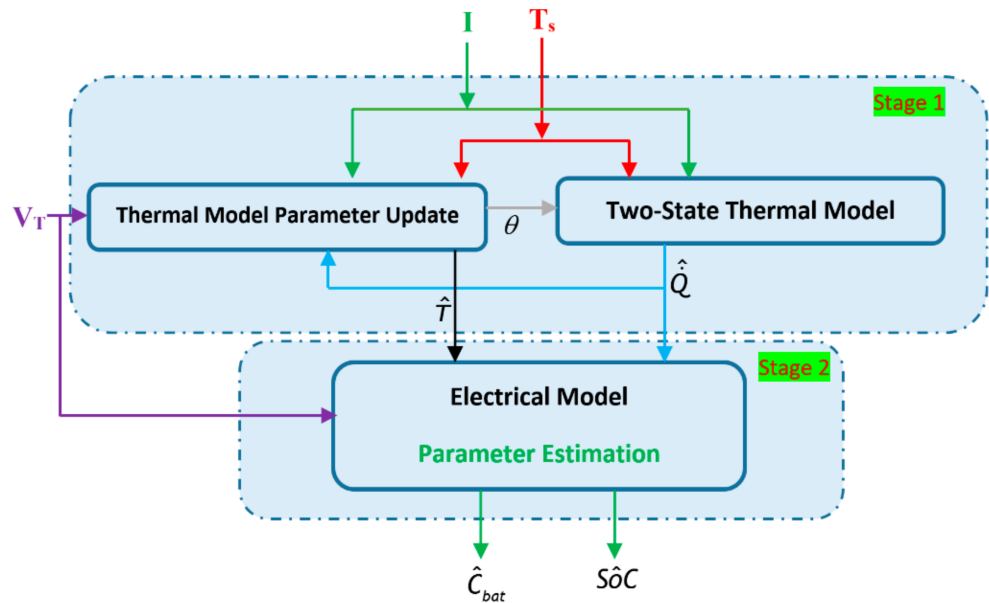


Figure 8. Cascaded online capacity estimation structure.

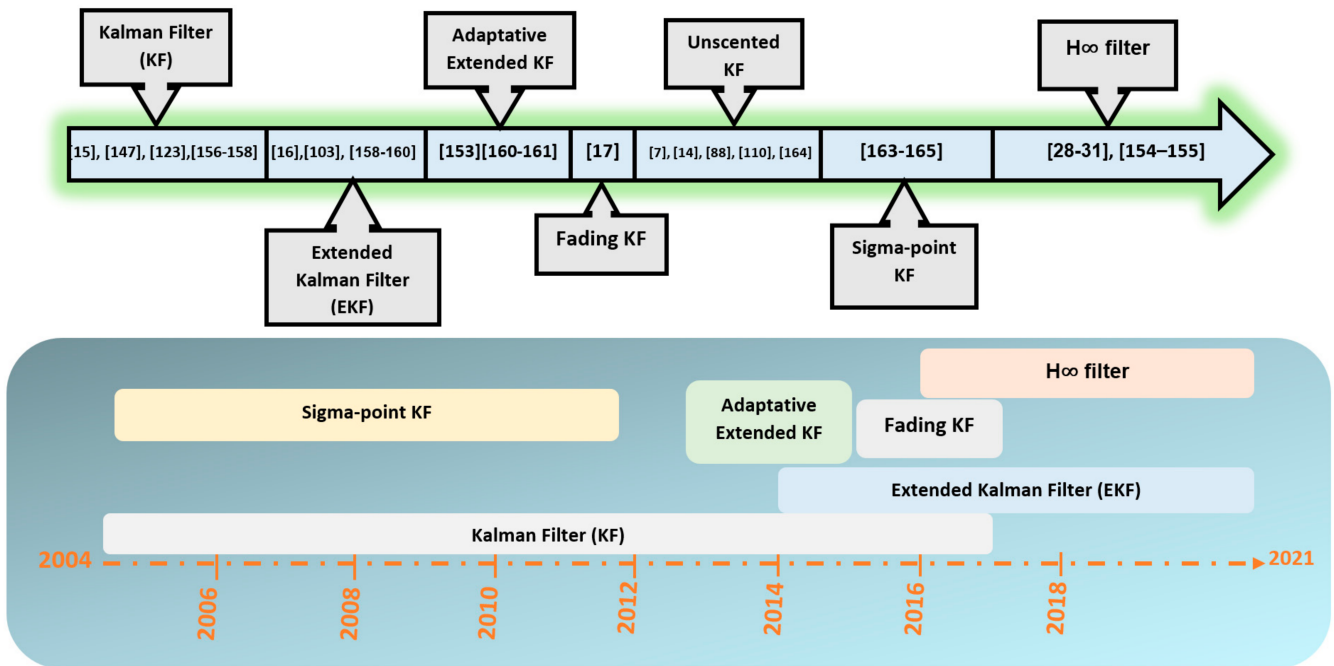
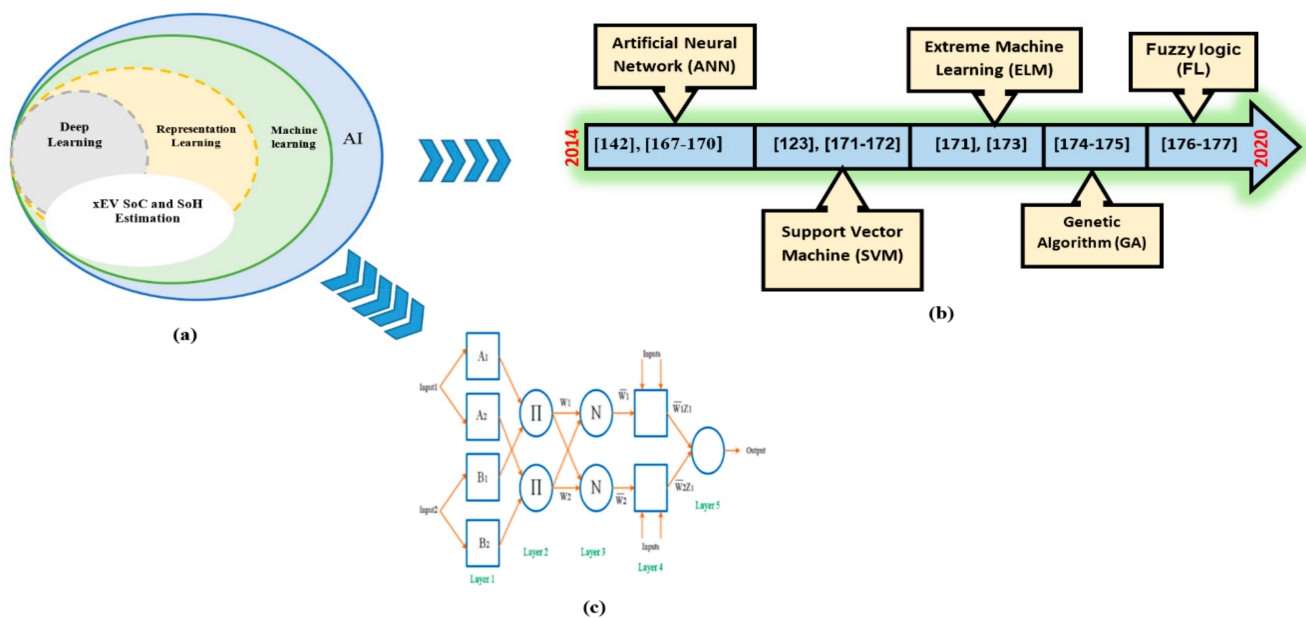


Figure 9. The adaptive filter algorithm for SoC estimation.



**Figure 10.** (a) The relation of EV SoC and SoH estimation in the field of artificial intelligence and machine learning. (b) The machine learning SoC estimation technique. (c) The general structure of the ANFIM.

To optimize the problems and the errors of SoC estimation, the particle swarm optimization (PSO) algorithm is added. Based on the different driving cycle experiments, and by considering noises and the battery test, the proposed technique demonstrates good performance for SoC estimation, even compared to Back-propagation neural network (BPNN) and Extend Kalman Filter (EKF). The dual-network fusion battery model was also used in [168] to evaluate the SoC of batteries based on the OCV approach. The concentration levels of the designed dual-network fusion battery model can also be used to define the properties of the electrochemical model parameters of the battery. The built-in dual-network fusion battery model is based on two neural network models wired in cascade. The first section is a linear neural network battery model that can be used to classify the parameters of the first or second order electrochemical model for the battery. The second part is a neural Back of Prorogation (BP) network used to capture the interaction between OCV and SoC. The authors in [169,170] used the input time delayed neural network to estimate the SoC and SoH of the lithium-ion batteries. Unlike other estimation techniques, this approach requires no previous knowledge of the parameters of the battery model. Alternatively, it uses ambient temperature fluctuations and past battery voltage and current data to precisely evaluate the SoC and SoH. The experimental results demonstrate its high precision, flexibility and robustness. The approach provided compensation for nonlinear trends in the characteristics of the batteries, such as hysteresis, variation due to electrochemical properties, and deterioration of the batteries due to age.

In [171–173], an enhanced dynamic model of a stationary lead-acid battery capable of forecasting its behavior under actual operating conditions is proposed. This model can simulate or precisely manage energy storage, particularly in PVS applications, and also in the case of electric or hybrid cars. The proposed model is reliable for any form of battery, under different conditions. This development also makes it beneficial for the model to monitor and measure all the properties of the battery, such as the charging state and the output voltage, and also to apply it in embedded systems for practical use in monitoring. A large number of samples are required for good estimation and, consequently, a high time of calculation is the main disadvantage observed in this technique.

The online SoC calculation approach with reducing pre-battery test details is the aim of the work proposed in [174], which does not include laboratory-based test data, but includes the relationship between OCV and SoC. [175,176] presents an intelligent SoC estimation technique for lithium-ion batteries. The model is built offline using an Adaptive

Neuro-Fuzzy Inference System (ANFIS). It calls the nonlinear characteristics of the cells, as provided by the manufacturer, which account for the relationship between the SoC cell and the OCV at various temperatures. The manufacturer's data are also used to model the cell characteristics of ANFIS in order to generate the SoC cell at some specific OCV and temperature within a specified range. The SoC pack is then measured. Compared to the Coulomb counting method, which is popular in the industry but remains inaccurate, the findings indicate a distinct advantage over the conventional Coulomb counting approach for the proposed ANFIS methodology. Figure 11 presents a comparative analysis of data-driven state estimation methods.

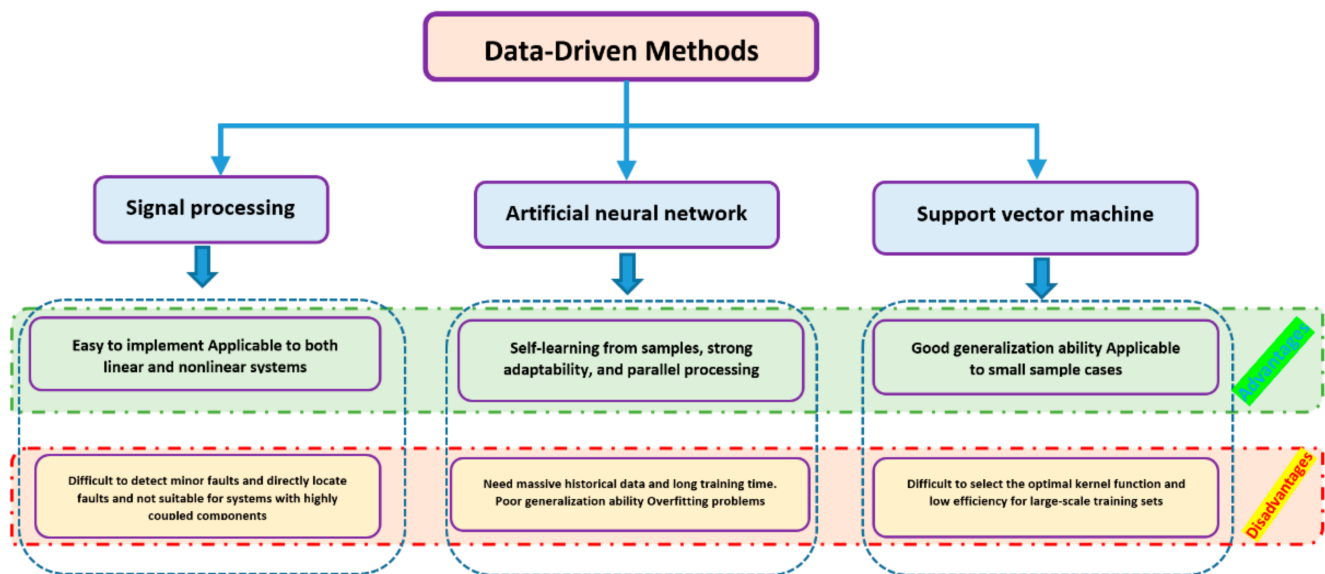


Figure 11. Advantages and disadvantages of data-driven state condition methods.

Today's most common disadvantage of the SoC estimation techniques of batteries in EV applications is that they do not consider the variation between the single cells and use the "averaged SoC" as the state-of-charge of the pack. In [177], a new approach for online pack SoC estimation and correction is suggested, incorporating the conventional SoC estimator and the adaptive neuro-fuzzy inference system (ANFIS). The standard KF based estimation method has been used first to estimate the "averaged SoC" of the battery pack, and then the ANFIS is used online to correct the "averaged" SoC calculation with cell differences and load current information. The effect of cell variations on SoC estimation is expressed in the blurry principles of the ANFIS, which is educated offline. The published research on machine learning techniques for SoC estimation is presented in Figure 10b. ANN has several benefits, such as the ability to model non-linear, the ability to learn, simultaneous data analysis and adaptation. This learning method is extended to a fuzzy system, which allows for an integrated modification of fuzzy standards. The typical configuration of the adaptive neuro-fuzzy inference method (ANFIM) is shown in Figure 10c [119].

According to the above analysis, the estimation error and the computation complexity of the SoC estimation methods currently being studied are roughly presented. The abscissa is the SoC estimation error, and the calculation complexity of the estimation methods is the coordinate.

### 3.2. The Internal Resistance Estimation Method

The main objective of the BMS is to improve the efficiency and lifespan of the battery. This is an important way to adjust the operating status of the battery by monitoring the differences in internal resistance between each cell. Battery setting techniques can be summarized in three categories: (1) sinusoidal scanning methods, e.g., electrochemical

impedance spectroscopy (EIS) [178]; (2) methods based on an equivalent electrical circuit model, e.g., Kalman Filter (KF), recursive least squares, genetic algorithms or particle swarm optimization [179–181]; and (3) methods based on electrochemical models such as uncoupled partial differential equations (PDEs) where, due to the large number of unknowns involved in the latter method, they are often excluded from the real-time use of BMS [182]. By comparison, due to their reliability and flexibility, electrical equivalent-circuit models are now at the core of virtually all conventional BMS algorithms where battery states such as state-of-charge (SoC), state of-power (SoP), state-of health (SoH), and state-of-function (SoF) have to be tested recursively online [129]. However, it makes it appear from the testing results that the operating conditions of the battery (temperature, charge/discharge rate, and aging effects) have a strong influence on the internal resistance of the battery and, therefore, the complexity of the equivalent battery circuit model must be considered as it reflects the dynamic characteristics of the battery. Consequently, it has been an empirical necessity to evaluate the EIR of the single cell and an entire case [183].

For the lithium-ion battery, the internal resistance ( $R_i$ ) includes the ohmic resistance ( $R_\Omega$ ) and the bias resistance ( $R_f$ ). Ohmic resistance is defined by the electrolyte, electrode materials, the separator resistance and the resistance of contact. Separator resistance ( $R_M$ ) is the electrolytic resistance of the efficient microporous membrane as the current passes through the electrolyte. The polarization resistance is defined by the bias during the electrochemical process, consisting of an electrochemical bias resistance and an intensity bias resistance. Under normal operating conditions, the ohm resistance primarily relates to the voltage decline, which is generally linear to the current density. Consequently, the ohm resistance is most interesting when determining the efficiency of a single cell. Different SoH are acquired based on data collection in a lithium-ion battery life cycle test experiment [183,184], and SoH Lithium-ion battery estimates are using incremental capacity analysis technique [185]. The correlation between EIR and SoH can be described by the EIR spectrum and the relationship between the level of degradation and the EIR is shown in [184].

In [186], the RLS model proposed by the recursive least squares algorithm can directly estimate the VOC and the  $R_s$  series resistance. The VOC-SoC search table, tabulated from experimental tests, is used to estimate the SoC. Based on the RLS method and the definition of the end of life of the battery, the SoH of the battery can be estimated as follows [67]:

$$SoH = \left( \frac{R_{S,dead} - R_s}{R_{S,dead} - R_{S,new}} \right) * 100\% \quad (7)$$

where,  $R_{S,dead}$  is the battery end of life series resistance, and  $R_{S,new}$  is the new battery series resistance. The scheme shown in the Figure 12 presents the model of life evolution based on the EIR.

The first approach consists in the use of observers (for example, the Kalman Filter is initially used in the determination of the charging state (SoC) and then extended to the determination of the resistance [187,188]) and neural networks [189], so that the technique is based on the monitoring of the evolution of the voltage drop over time to update the estimation of the RS resistance series [190]. In [191] the coefficients, which may vary depending on the effects of aging and the corresponding law of variation, must be established in order to eliminate the effects of temperature, regardless of aging. Fuzzy logic algorithms [192] sometimes require significant time for computing and memory allocation and therefore become impractical in some applications. The second idea is to study the ratio of voltage drops to current variations when they occur during normal cellular operation. These methods are also used for sudden discharges, which can be assumed as controlled pulses [191].

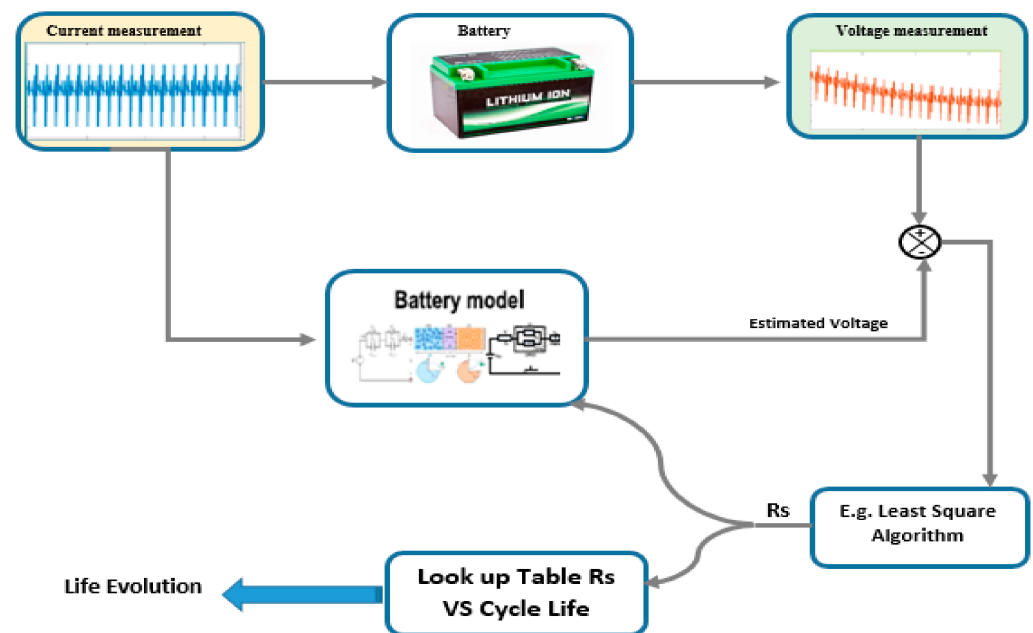


**Figure 12.** Relationship between the battery degradation level and EIR.

The method proposed in [193] is more accurate than the Constant Current Test (CCT) method because the CCT method produces a much weaker result than the hybrid power pulse characterization (HPPC) method. The greatest variation between these two methods is as high as 55.64% at the end of the test, which proves that the proposed method greatly improves accuracy compared to the CCT method. Considering the characteristics of the lithium-ion battery, these methods of analysis and the simplified equivalent model shall be used in the real-time evolution of the state of the battery taking into consideration all parameters affected in the state of the health of the battery. Based on these general ideas about the algorithms and techniques used to estimate the internal resistance of the battery and the rapid assessment of the condition of the transplanted algorithms, and the online identification of the internal resistance, further analytical studies will be worth doing in future work.

#### 4. The Aging of LiB and Temperature Dependence

Aging is the entire process of deterioration of the electrochemical properties of the accumulator due to degradation at the level of the anode, cathode, electrolyte or separator. Concrete aging is demonstrated by a loss of capacity and an increase in the cell's internal resistance. It's well known that the aging of the batteries affected the precision of the SoC estimation. The main factors leading the aging are the degradation of internal resistance and performance, as well as the fading of available power. As a result, research into the fault mechanisms, fault characteristics, and diagnostic methods for LiBs is needed. The weaknesses in LiBs are shown in Figure 13. Inherent failures, improper use, and harsh conditions all cause LiBs faults. Condition monitoring of LiBs is problematic due to these internal and external causes, as well as their difficult coupling relationship. In general, LiBs faults are covered, making it impossible to assess early fault conditions clearly and precisely using only voltage, current, and temperature signals. Each fault presents a different hazard to a LIBS. Battery failures could compromise device performance and even result in disastrous events like battery fires and explosions.

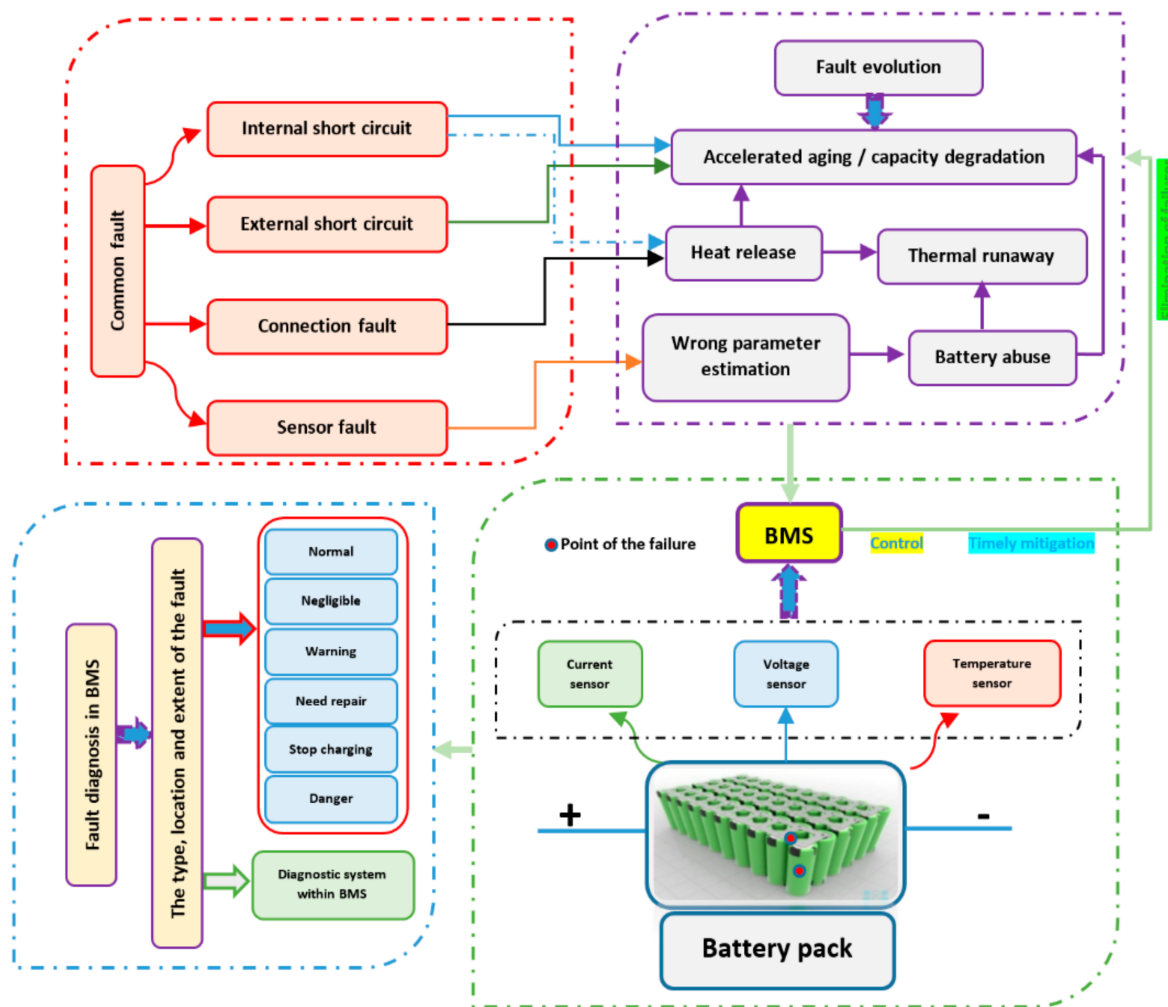


Figure 13. Analysis of the reasons for LiB aging.

The key factors of aging of the Li-ion batteries are the evaporation of the solid electrolyte interphase (SEI), deposition of the anode, dissolution of the metal from the anode, depletion of active material and lithium plating [16]. The analysis of the causes for the aging of the battery is illustrated in Figure 14.

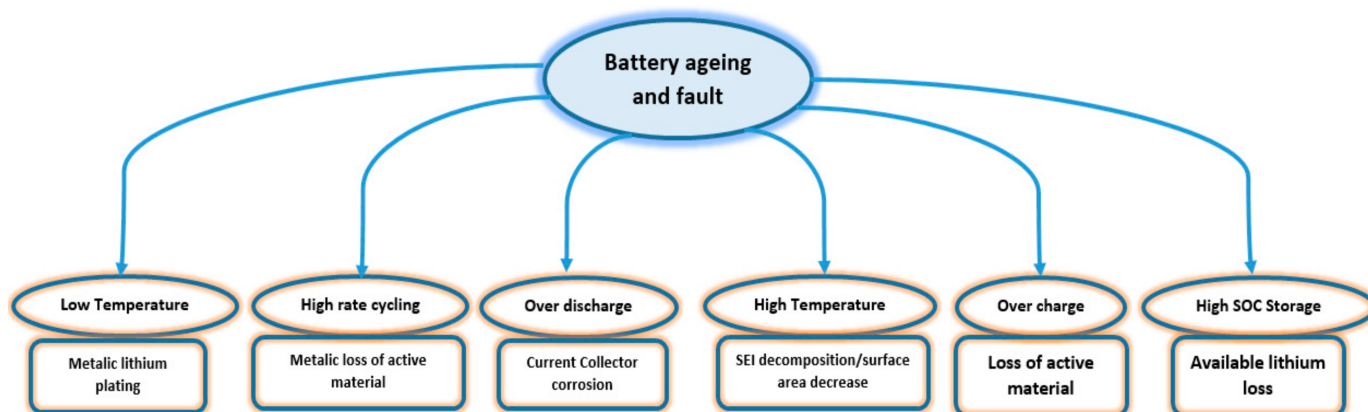


Figure 14. Analysis of the reasons for LiB aging.

Electrochemical impedance spectroscopy (EIS) is a technique used to measure the internal impedance of a battery over a frequency range. The EIS is a powerful tool for

understanding the internal state of the battery and its aging mechanism. EIS is useful for determining the residual useful life (RUL) and health (SoH) of the battery due to aging [194]. In most cases, the hybrid data-driven and model-based technique produces more accurate RUL prediction findings. However, such hybridization is more complicated and necessitates greater computing skill, making it challenging for online practical applications. Aside from combining data-driven and model-based approaches, other data-driven methods may be combined to increase accuracy and reliability of the RUL prediction results. Few calculation methods have been developed to measure the impedance of the battery. Analysis of Lissajous, phase-sensitive detection and single/multiple-frequency transformation of Fourier are some theoretical approaches [195–203].

A new technique based on the hybrid battery configuration technique for the online battery state of power (SoP) prediction uses the identification of the pseudo-random binary sequence (PRBS) of the resistive battery parameters required for the SoP prediction, since the battery has been rested for at least 30 min before the charge is started [196]. A method for predicting the initial short-circuit current for lead-acid batteries [204] has been also proposed. Mao et al. [205] presented the Sensor Selection Algorithm, by considering sensors' sensitivities to various failure modes and corresponding degradation rates, which were applied in practical fuel cell membrane polymer electrolyte systems for online fault diagnosis.

Yang et al. [206] presented an approach based on an ESC fault diagnostic model using a fractional order model. Chen et al. [207] was tested to estimate the maximum temperature rise of the ESC fault. While considerable advances have been made in fault diagnostic methodology, there is no procedure for diagnosing internally and externally short-circuit defects in LiB packs used in EVs that may have severe implications. Spotnitz and Franklin [208] presented the abuse tests for LiBs and their components, including the oven test [209], nail penetration [210], crushing test and short circuits, and developed models to describe the behavior of batteries under conditions of abuse [211]. The variation in the internal properties of cells due to manufacturing processes partly explains the life-span differences that exist between cells. Cell ages are observed to be faster when the current demand has an AC component, the frequency of which appears to influence cell damage [57]. Unfortunately, the causes of the phenomenon remain unexplained [57]. Typically, we will define that the accumulator has reached the end of its useful life when we measure a relative increase in internal resistance of twice its initial value or when the capacity falls below 80% of its original capacity [58]. However, there is no standardized way to define the SoH. An advanced aging methodology for observing calendar aging and cyclic aging, similar to the work of [59], was developed in [60].

As far as contingent temperature is concerned, the online power calculation scheme for Li-ion batteries is shown in Figure 8.

The key breakthrough is: (1) the use of thermal dynamics to estimate the battery capacity; and (2) the development of a hierarchical estimation algorithm with validated convergence properties. The algorithm composes of two phases of cascade operation. The first stage estimates the core temperature of the battery and the production of heat based on a two-state thermal model, and the second stage provides an estimate of the core temperature and the production of heat to estimate the SoC and capacity [36]. Charge and discharge temperatures show a clear relationship between the generation of temperatures and the aging of the batteries, and the constant ambient temperature during discharge mostly acts as an initial condition [69].

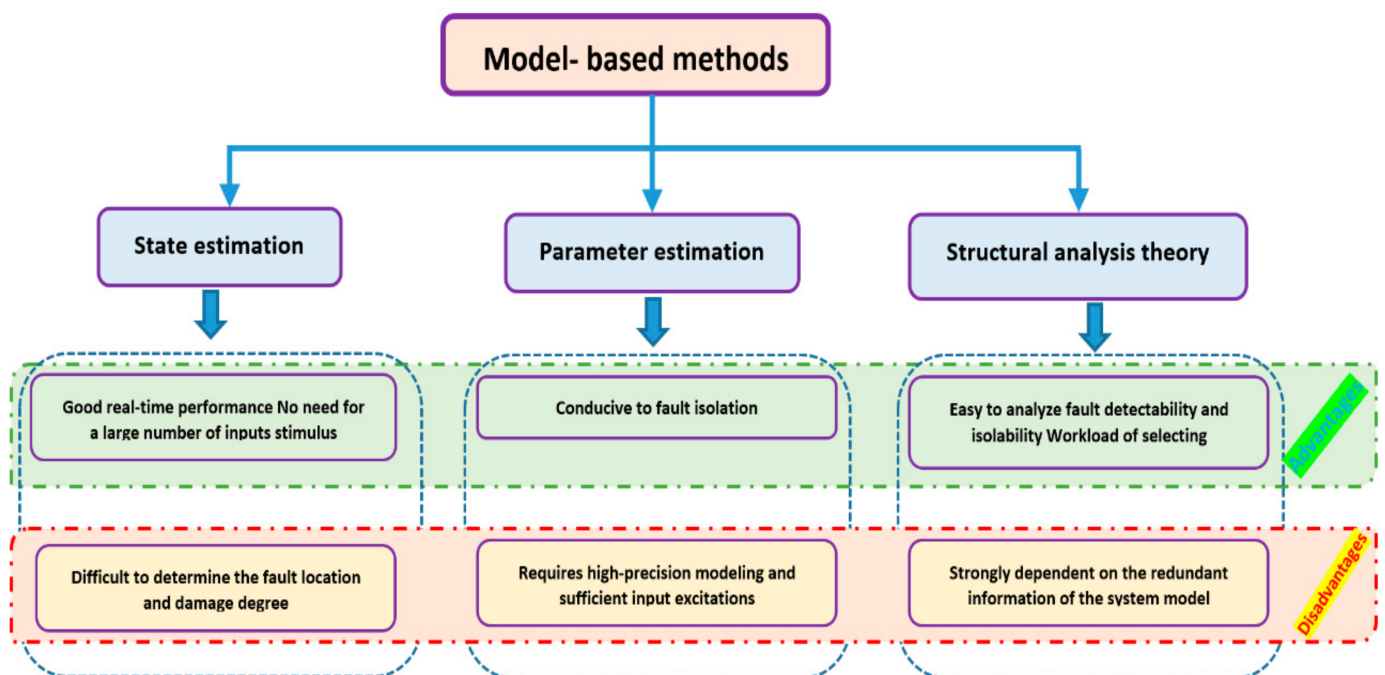


Figure 15. Advantages and disadvantages of model-based state condition methods [154,155,211].

The State of the Health (SoH) with its different definitions is a difficult problem too, and a critical factor in the battery energy storage system, especially when it comes to accuracy and reliability. In [212] several SoH battery diagnostic and monitoring methods are presented with diverse technologies and applications. The methods are classified in terms of experimental implementation method and adaptive models. The diagnostic model proposed in [213] is a model allowing to estimate SoC and SoH online. The strong point is that it does not require the interruption of the operation of the system, contrary to the DC and EIS characterization methods. The charging mode of the battery is not considered, so the robustness of the technique is shown in discharging mode, and high performance is shown also for different operating temperatures, discharging currents, and also for different aging conditions.

The State of Energy (SoE) of lithium-ion batteries is an important measurement index for energy storage systems in electric vehicles, hybrid electric vehicles, and smart grids. It provides the basis for energy deployment, load balancing and energy security for complex energy systems. The crucial goal is to obtain a precise and reliable SoE estimation. To obtain a good and accurate estimation of SoE it should be remembered that:

1. The energy of the battery is very much affected, and influenced, by its OCV;
2. OCV model must take the temperature into account;
3. The total energy of the battery is influenced by the ambient temperature and load current;
4. The errors caused by current or voltage measurement noises have to be considered.

In [9], a model-based estimation is developed based on two filters, one to identify the battery model parameters by EKF, using the real time acquisition of the battery current and voltage, and the other to estimate the battery SoE by PF. The experimental validation shows the robustness and reliability of this technique by obtaining an error almost equal to 4% for the estimation of SoE, even under the consideration of the battery aging. The other parameters of the battery are identified in real-time. In the same line, it was proposed in [214] that an online SoE estimation approach based on the first-order RC equivalent circuit model, and the Bayesian training algorithm, was used to evaluate the precision and robustness of the SoE estimation. For the electrochemical and thermodynamics coupled equivalent circuit model (ECM), several works have been developed not just to provide an

accurate and reliable state monitoring, but also for the effective thermal management of lithium-ion batteries. Based on a thermal coupled equivalent circuit model, an integrated artificial neural network technique is developed in [215] to evaluate the electrical and thermal properties of lithium-ion batteries in terms of accuracy and reliability. In the thermal model, reversible and irreversible heat production processes are implemented. The electrical and thermal parameters are identified by means of the least square algorithm technique, and the relationship between them and temperature and SoC is determined by an artificial neural network.

Irregular aging in batteries is mainly due to thermal imbalances and even to the state of charge. An electro-thermal control of a multi-level modular battery-based converter is presented in [216] to solve this problem. The main objective of the coupled control is to include the thermal and SoC balancing at the same time, and the battery terminal voltage control. This decomposition allows the implementation of a constrained linear quadratic model predictive control scheme to solve the balancing problem. In [217], a hybrid electrochemical, heat generation, and thermal model for large prismatic cells are developed to predict in real time the core temperature and terminal voltage to improve the reliability of a BMS at various operating conditions.

The developed model coupled three sub-models: an electrochemical model, heat generation model, and thermal model. Some accurate methods also use a battery state of the health (SoH). As it is so critical, it is used to determine the replacement time of the battery or to evaluate the driving mileage. The authors in [218] have demonstrated how SoH can be estimated in more practical environments where batteries must support real-world driving patterns. They proposed a data-driven approach to track SoH using plausible BMS data such as current, voltage and temperature while making use of their historical distributions. In [219–221], another data-driven method is developed to evaluate the SoC of li-ion batteries using a Recurrent Neural Network (RNN) with a Long Short-Term Memory (LSTM). This LSTM-RNN has the ability to estimate the SoC accurately without using the model of the battery or filters. Like all machine learning techniques, it took advantage of the training taken under different conditions to train the LSTM-RNN model on datasets recorded at different ambient temperatures, resulting in a single network that can correctly estimate the SoC under different ambient temperature conditions. Figure 16 covers the recent literature about estimating the state parameters of the batteries of electric vehicles and incorporating the effect of the variation of temperature as it has a major effect on systems' life and battery performance, especially in cold climates.

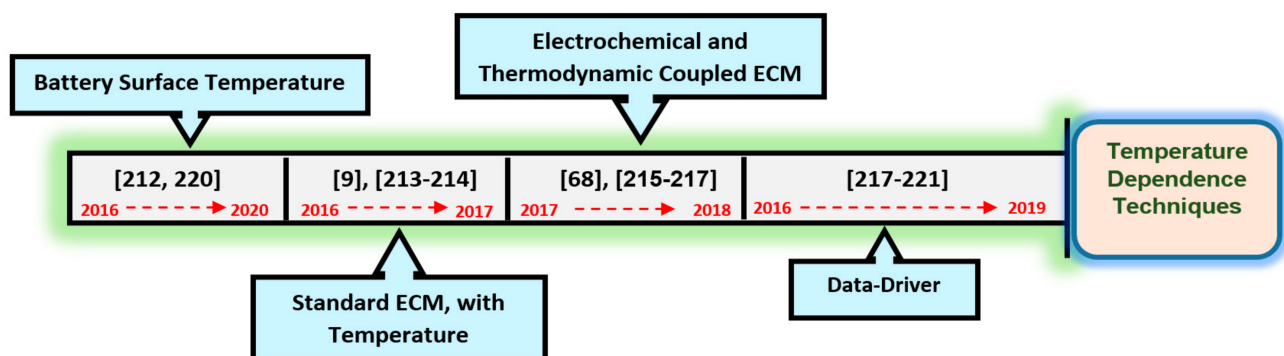


**Figure 16.** Lithium-ion battery of electric vehicles state parameters estimation techniques, incorporating the effect of the variation in temperature.

## 5. Conclusions

This paper presents a detailed review of various SoC estimation strategies intended for developing and installing an electrical vehicle BMS, which has been a challenging task due to complicated electrochemical reactions and degraded efficiency, depending on a variety of factors. Owing to the high demand for electric vehicles, the range of battery technologies

will be further increased and since the electrochemical materials and efficiency of all types of batteries are distinct, this will add a great deal of complexity and difficulties to the overall SoC estimation. However, periodic readjustment is also required, as accumulated errors do not disappear. The estimation approach based on the ECM + KF group should give greater attention to optimizing the model's voltage drift using a more sophisticated estimation methodology. The estimation method based on machine learning could further train the model with real-world data, or sometimes-unmonitored machine learning is necessary because using real-world data it is hard to obtain reliable SoCs. On the other hand, the internal resistance of the battery is among the most critical characteristic parameters for measuring and improving the performance and lifetime of the battery. Increasing the internal resistance of the battery will lower the discharge voltage of the battery, reduce the discharge time and have a significant effect on the battery's power characteristics. Internal resistance is one of the most significant metrics for calculating battery efficiency and life. Raising the internal resistance of the battery will increase the discharge voltage of the device, shorten the discharge time and have a direct effect on the battery's performance characteristics.

The last interesting aspect of this analysis was the recent literature survey on the calculation of the battery status parameters of EVs and the integration of the effect of temperature variability, as this has a major impact on battery life and efficiency, especially in cold climates. Temperatures beyond the optimal operating range intensify the aging of the batteries and, when the cells mature, the internal resistance decreases, resulting in permanent heat losses. Early detection of temperature distribution changes with the related temperature-dependent battery-packing model, which can be used as input to the effective thermal management system.

These suggestions offer a remarkable contribution to the evolution of the state of the battery by considering all the variables that may influence the state of operation or the state of health. Future work will focus on the use of ECM strength and order, of relatively simple models, and the constraints are that they cannot be shown the kinetics of internal reaction, as well as the degradation of the capacity and aging path of the batteries. Consequently, by mixing various types of battery models and methodologies with a well-designed fusion rule, a fused system will provide strong predictive efficiency in unknown aging, operating environments and conditions, and battery materials.

**Author Contributions:** Conceptualization, K.L. and A.J.M.C.; methodology, K.L. and A.J.M.C.; software, K.L.; validation, K.L.; formal analysis, K.L.; investigation, K.L.; resources, A.J.M.C.; data curation, K.L.; writing—original draft preparation, K.L.; writing—review and editing, A.J.M.C.; visualization, K.L.; supervision, A.J.M.C.; project administration, A.J.M.C.; funding acquisition, A.J.M.C. All authors have read and agreed to the published version of the manuscript.

**Funding:** This work was supported by the European Regional Development Fund (ERDF) through the Operational Programme for Competitiveness and Internationalization (COMPETE 2020), under Project POCI-01-0145-FEDER-029494, and by National Funds through the FCT—Portuguese Foundation for Science and Technology, under Projects PTDC/EEI-EEE/29494/2017, UIDB/04131/2020, and UIDP/04131/2020.

**Conflicts of Interest:** The authors declare no conflict of interest.

## References

1. Sulaiman, N.; Hannan, M.A.; Mohamed, A.; Majlan, E.H.; Daud, W.R.W. A review on energy management system for fuel cell hybrid electric vehicle: Issues and challenges. *Renew. Sustain. Energy Rev.* **2015**, *52*, 802–814. [[CrossRef](#)]
2. Essl, C.; Seifert, L.; Rabe, M.; Fuchs, A. Early Detection of Failing Automotive Batteries Using Gas Sensors. *Batteries* **2021**, *7*, 25. [[CrossRef](#)]
3. Ibrahim, A.; Jiang, F. The electric vehicle energy management: An overview of the energy system and related modeling and simulation. *Renew. Sustain. Energy Rev.* **2021**, *144*, 111049. [[CrossRef](#)]
4. Gabbar, H.A.; Othman, A.M.; Abdussami, M.R. Review of Battery Management Systems (BMS) Development and Industrial Standards. *Technologies* **2021**, *9*, 28. [[CrossRef](#)]

5. Xing, Y.; Ma, E.W.M.; Tsui, K.L.; Pecht, M. Battery management systems in electric and hybrid vehicles. *Energies* **2011**, *4*, 1840–1857. [[CrossRef](#)]
6. Eichl, H.R.; Ojha, U.; Baronti, F.; Chow, M.Y. Battery management system: An overview of its application in the smart grid and electric vehicles. *IEEE Ind. Electron. Mag.* **2013**, *7*, 4–15. [[CrossRef](#)]
7. Zou, C.; Manzie, C.; Nešić, D.; Kallapur, A.G. Multi-time-scale observer design for state-of-charge and state-of-health of a lithium-ion battery. *J. Power Sources* **2016**, *335*, 121–130. [[CrossRef](#)]
8. Dong, G.; Chen, Z.; Wei, J.; Zhang, C.; Wang, P. An online model-based method for state of energy estimation of lithium-ion batteries using dual filters. *J. Power Sources* **2016**, *301*, 277–286. [[CrossRef](#)]
9. He, H.; Zhang, Y.; Xiong, R.; Wang, C. A novel Gaussian model based battery state estimation approach: State-of-Energy. *Appl. Energy* **2015**, *151*, 41–48. [[CrossRef](#)]
10. Zhai, G.; Liu, S.; Wang, Z.; Zhang, W.; Ma, Z. State of Energy Estimation of Lithium Titanate Battery for Rail Transit Application. *Energy Procedia* **2017**, *105*, 3146–3151. [[CrossRef](#)]
11. Li, Y.; Chattopadhyay, P.; Ray, A.; Rahn, C.D. Identification of the battery state-of-health parameter from input-output pairs of time series data. *J. Power Sources* **2015**, *285*, 235–246. [[CrossRef](#)]
12. Feng, T.; Yang, L.; Zhao, X.; Zhang, H.; Qiang, J. Online identification of lithium-ion battery parameters based on an improved equivalent-circuit model and its implementation on battery state-of-power prediction. *J. Power Sources* **2015**, *281*, 192–203. [[CrossRef](#)]
13. Beck, D.; Dechent, P.; Junker, M.; Sauer, D.U.; Dubarry, M. Inhomogeneities and Cell-to-Cell Variations in Lithium-Ion Batteries, a Review. *Energies* **2021**, *14*, 3276. [[CrossRef](#)]
14. Zheng, Y.; Ouyang, M.; Han, X.; Lu, L.; Li, J. Investigating the error sources of the online state of charge estimation methods for lithium-ion batteries in electric vehicles. *J. Power Sources* **2018**, *377*, 161–188. [[CrossRef](#)]
15. Yang, K.; Tang, Y.; Zhang, Z. Parameter Identification and State-of-Charge Estimation for Lithium-Ion Batteries Using Separated Time Scales and Extended Kalman Filter. *Energies* **2021**, *14*, 1054. [[CrossRef](#)]
16. Hu, X.; Li, S.; Peng, H.; Sun, F. Robustness analysis of State-of-Charge estimation methods for two types of Li-ion batteries. *J. Power Sources* **2012**, *217*, 209–219. [[CrossRef](#)]
17. Lim, K.; Bastawrous, H.A.; Duong, V.-H.; See, K.W.; Zhang, P.; Dou, S.X. Fading Kalman filter-based real-time state of charge estimation in LiFePO<sub>4</sub> battery-powered electric vehicles. *Appl. Energy* **2016**, *169*, 40–48. [[CrossRef](#)]
18. Gao, Z.C.; Chin, C.S.; Toh, W.D.; Chiew, J.; Jia, J. State-of-charge estimation and active cell pack balancing design of lithium battery power system for smart electric vehicle. *J. Adv. Transp.* **2017**, *2017*, 1–14. [[CrossRef](#)]
19. Jia, J.; Lin, P.; Chin, C.S.; Toh, W.D.; Gao, Z.; Lyu, H.; Cham, Y.T.; Mesbahi, E. Multirate strong tracking extended Kalman filter and its implementation on lithium iron phosphate (LiFePO<sub>4</sub>) battery system. In Proceedings of the IEEE International Conference on Power Electronics and Drive Systems, Sydney, NSW, Australia, 9–12 June 2015; pp. 640–645.
20. Tang, X.; Liu, B.; Gao, F.; Lv, Z. State-of-charge estimation for Li-Ion power batteries based on a tuning free observer. *Energies* **2016**, *9*, 675. [[CrossRef](#)]
21. Torai, S.; Nakagomi, M.; Yoshitake, S.; Yamaguchi, S.; Oyama, N. State-of-health estimation of LiFePO<sub>4</sub>/graphite batteries based on a model using differential capacity. *J. Power Sources* **2016**, *306*, 62–69. [[CrossRef](#)]
22. Ning, B.; Xu, J.; Cao, B.; Wang, B.; Xu, G. A sliding mode observer SOC estimation method based on parameter adaptive battery model. *Energy Procedia* **2016**, *88*, 619–626. [[CrossRef](#)]
23. Zhong, Q.; Zhong, F.; Cheng, J.; Li, H.; Zhong, S. State of charge estimation of lithium-ion batteries using fractional order sliding mode observer. *ISA Trans.* **2017**, *66*, 448–459. [[CrossRef](#)]
24. Kim, I.S. The novel state of charge estimation method for lithium battery using sliding mode observer. *J. Power Sources* **2006**, *163*, 584–590. [[CrossRef](#)]
25. Ma, Y.; Li, B.; Xie, Y.; Chen, H. Estimating the State of Charge of Lithium-ion Battery based on Sliding Mode Observer. *IFAC Papers Online* **2016**, *49*, 54–61. [[CrossRef](#)]
26. Zhang, F.; Liu, G.; Fang, L. A battery state of charge estimation method using sliding mode observer. In Proceedings of the 2008 World Congress on Intelligent Control and Automation, Chongqing, China, 25–27 June 2008; pp. 989–994.
27. Du, J.; Liu, Z.; Wang, Y.; Wen, C. An adaptive sliding mode observer for lithium-ion battery state of charge and state of health estimation in electric vehicles. *Control Eng. Pract.* **2016**, *54*, 81–90. [[CrossRef](#)]
28. Lin, C.; Mu, H.; Xiong, R.; Shen, W. A novel multi-model probability battery state of charge estimation approach for electric vehicles using H-infinity algorithm. *Appl. Energy* **2016**, *166*, 76–87. [[CrossRef](#)]
29. Mu, H.; Xiong, R.; Sun, F. A novel multi-model probability based battery state-of-charge fusion estimation approach. *Energy Procedia* **2016**, *88*, 840–846. [[CrossRef](#)]
30. Zhu, Q.; Xiong, N.; Yang, M.-L.; Huang, R.-S.; Hu, G.-D. State of Charge Estimation for Lithium-Ion Battery Based on Nonlinear Observer: An  $H_\infty$  Method. *Energies* **2017**, *10*, 679. [[CrossRef](#)]
31. Chen, N.; Zhang, P.; Dai, J.; Gui, W. Estimating the State-of-Charge of Lithium-Ion Battery Using an H-Infinity Observer Based on Electrochemical Impedance Model. *IEEE Access* **2020**, *8*, 26872–26884. [[CrossRef](#)]
32. Hu, X.; Sun, F.; Zou, Y. Estimation of State of Charge of a Lithium-Ion Battery Pack for Electric Vehicles Using an Adaptive Luenberger Observer. *Energies* **2010**, *3*, 1586–1603. [[CrossRef](#)]

33. Bartlett, A.; Marcicki, J.; Onori, S.; Rizzoni, G.; Yang, X.G.; Miller, T. Electrochemical model-based state of charge and capacity estimation for a composite electrode lithium-ion battery. *IEEE Trans. Control Syst. Technol.* **2016**, *24*, 384–399. [[CrossRef](#)]
34. Moura, J.N.; Chaturvedi, N.A.; Krstić, M. Adaptive partial differential equation observer for battery state-of-charge/state-of-health estimation via an electrochemical model. *J. Dyn. Syst. Meas. Control* **2014**, *136*, 11–15. [[CrossRef](#)]
35. Klass, V.; Behm, M.; Lindbergh, G. Evaluating real-life performance of lithium-ion battery packs in electric vehicles. *J. Electrochem. Soc.* **2012**, *159*, 1856–1860. [[CrossRef](#)]
36. Charkhgard, M.; Zarif, M.H. Design of adaptive H $\infty$  filter for implementing on state-of-charge estimation based on battery state-of-charge-varying modelling. *Power Electron. IET* **2015**, *8*, 1825–1833. [[CrossRef](#)]
37. Xia, B.; Chen, Z.; Mi, C. External Short Circuit Fault Diagnosis for Lithium-Ion Batteries. In Proceedings of the IEEE Transportation Electrification Conference and Expo (ITEC), Dearborn, MI, USA, 15–18 June 2014; pp. 1–7.
38. Chiu, K.; Lin, C.; Yeh, S.; Lin, Y.; Chen, K. An electrochemical modeling of lithium-ion battery nail penetration. *J. Power Sources* **2014**, *251*, 254–263. [[CrossRef](#)]
39. Kalawoun, J.; Biletska, K.; Suard, F.; Montaru, M. From a novel classification of the battery state of charge estimators toward a conception of an ideal one. *J. Power Sources* **2015**, *279*, 694–706. [[CrossRef](#)]
40. Li, J.; Klee Barillas, J.; Guenther, C.; Danzer, M.A. A comparative study of state of charge estimation algorithms for LiFePO<sub>4</sub> batteries used in electric vehicles. *J. Power Sources* **2013**, *230*, 244–250. [[CrossRef](#)]
41. Burgos, C.; Sáez, D.; Orchard, M.E.; Cárdenas, R. Fuzzy modelling for the state-of-charge estimation of lead-acid batteries. *J. Power Sources* **2015**, *274*, 355–366. [[CrossRef](#)]
42. Oh, K.-Y.; Samad, N.A.; Kim, Y.; Siegel, J.B.; Stefanopoulou, A.G.; Epureanu, B.I. A novel phenomenological multi-physics model of Li-ion battery cells. *J. Power Sources* **2016**, *326*, 447–458. [[CrossRef](#)]
43. Zhang, M.; Fan, X. Review on the State of Charge Estimation Methods for Electric Vehicle Battery. *World Electr. Veh. J.* **2020**, *11*, 23. [[CrossRef](#)]
44. Nejad, S.; Gladwin, D.T.; Stone, D.A. A systematic review of lumped-parameter equivalent circuit models for real-time estimation of lithium-ion battery states. *J. Power Sources* **2016**, *316*, 183–196. [[CrossRef](#)]
45. Zhang, R.; Xia, B.; Li, B.; Cao, L.; Lai, Y.; Zheng, W.; Wang, H.; Wang, W. State of the Art of Lithium-Ion Battery SOC Estimation for Electrical Vehicles. *Energies* **2018**, *11*, 1820. [[CrossRef](#)]
46. Tsang, K.M.; Sun, L.; Chan, W.L. Identification and modelling of Lithium ion battery. *Energy Conver. Manag.* **2010**, *51*, 2857–2862. [[CrossRef](#)]
47. Saariluoma, H.; Piironen, A.; Unt, A.; Hakanen, J.; Rautava, T.; Salminen, A. Overview of Optical Digital Measuring Challenges and Technologies in Laser Welded Components in EV Battery Module Design and Manufacturing. *Batteries* **2020**, *6*, 47. [[CrossRef](#)]
48. Saw, L.H.; Ye, Y.; Tay, A.A. Integration issues of lithium-ion battery into electric vehicles battery pack. *J. Clean. Prod.* **2016**, *113*, 1032–1045. [[CrossRef](#)]
49. Al-Turjman, F.; Malekloo, A. Smart parking in IoT-enabled cities: A survey. *Sustain. Cities Soc.* **2019**, *49*, 101608. [[CrossRef](#)]
50. Oswal, M.; Paul, J.; Zhao, R. *A Comparative Study of Lithium-Ion Batteries*; Tech. Rep. AME 578 Project; University of Southern California: Los Angeles, CA, USA, 2010.
51. Pramanik, P.; Sinhababu, N.; Mukherjee, B.; Padmanaban, S.; Maity, A.; Upadhyaya, B.; Holm-Nielsen, J.; Choudhury, P. Power Consumption Analysis, Measurement, Management, and Issues: A State-of-the-Art Review of Smartphone Battery and Energy Usage. *IEEE Access* **2019**, *7*, 182113–182172. [[CrossRef](#)]
52. Arora, S.; Shen, W.; Kapoor, A. Review of mechanical design and strategic placement technique of a robust battery pack for electric vehicles. *Renew. Sustain. Energy Rev.* **2016**, *60*, 1319–1331. [[CrossRef](#)]
53. Pizarro-Carmona, V.; Cortés-Carmona, M.; Palma-Behnke, R.; Calderón-Muñoz, W.; Orchard, M.E.; Estévez, P.A. An Optimized Impedance Model for the Estimation of the State-of-Charge of a Li-Ion Cell: The Case of a LiFePO<sub>4</sub> (ANR26650). *Energies* **2019**, *12*, 681. [[CrossRef](#)]
54. He, H.; Xiong, R.; Fan, J. Evaluation of lithium-ion battery equivalent circuit models for state of charge estimation by an experimental approach. *Energies* **2011**, *4*, 582–598. [[CrossRef](#)]
55. Hossain, E.; Murtaugh, D.; Mody, J.; Faruque, H.; Sunny, S.; Mohammad, N. A Comprehensive Review on Second-Life Batteries: Current State, Manufacturing Considerations, Applications, Impacts, Barriers & Potential Solutions, Business Strategies, and Policies. *IEEE Access* **2019**, *7*, 73215–73252.
56. Wang, Q.; Jiang, B.; Li, B.; Yan, Y. A critical review of thermal management models and solutions of lithium-ion batteries for the development of pure electric vehicles. *Renew. Sustain. Energy Rev.* **2016**, *64*, 106–128. [[CrossRef](#)]
57. Seaman, A.; Dao, T.-S.; McPhee, J. A survey of mathematics-based equivalent-circuit and electrochemical battery models for hybrid and electric vehicle simulation. *J. Power Sources* **2014**, *256*, 410–423. [[CrossRef](#)]
58. Lee, K.-J.; Smith, K.; Pesaran, A.; Kim, G.-H. Three dimensional thermal-, electrical-, and electrochemical-coupled model for cylindrical wound large format lithium-ion batteries. *J. Power Sources* **2013**, *241*, 20–32. [[CrossRef](#)]
59. Randles, J.E.B. Kinetics of rapid electrode reactions. *Discuss. Faraday Soc.* **1947**, *1*, 11–19. [[CrossRef](#)]
60. Shepherd, C.M. Design of primary and secondary cells: II. An equation describing battery discharge. *J. Electrochem. Soc.* **1965**, *112*, 657–664. [[CrossRef](#)]
61. Bernardi, D.; Pawlikowski, E.; Newman, J. A general energy balance for battery systems. *J. Electrochem. Soc.* **1985**, *132*, 5–12. [[CrossRef](#)]

62. Shen, P.; Ouyang, M.; Lu, L.; Li, J.; Feng, X. The co-estimation of state of charge, state of health, and state of function for lithium-ion batteries in electric vehicles. *IEEE Trans. Veh. Technol.* **2018**, *67*, 92–103. [[CrossRef](#)]
63. Lai, X.; Gao, W.; Zheng, Y.; Ouyang, M.; Li, J.; Han, X.; Zhou, L. A comparative study of global optimization methods for parameter identification of different equivalent circuit models for Li-ion batteries. *Electrochim. Acta* **2019**, *295*, 1057–1066. [[CrossRef](#)]
64. Yang, J.; Xia, B.; Huang, W.; Fu, Y.; Mi, C. Online state-of-health estimation for lithium-ion batteries using constant-voltage charging current analysis. *Appl. Energy* **2018**, *212*, 1589–1600. [[CrossRef](#)]
65. Zhang, X.; Wang, Y.; Liu, C.; Chen, Z. A novel approach of battery pack state of health estimation using artificial intelligence optimization algorithm. *J. Power Sources* **2018**, *376*, 191–199. [[CrossRef](#)]
66. Shen, P.; Ouyang, M.; Lu, L.; Li, K.; Feng, X. State of Charge, State of Health and State of Function Co-Estimation of Lithium-Ion Batteries for Electric Vehicles. In Proceedings of the IEEE Vehicle Power and Propulsion Conference (VPPC), Hangzhou, China, 17–20 October 2016; pp. 1–5.
67. Gholizadeh, M.; Salmasi, F.R. Estimation of state of charge, unknown nonlinearities, and state of health of a lithium-ion battery based on a comprehensive unobservable model. *IEEE Trans. Ind. Electron.* **2014**, *61*, 1335–1344. [[CrossRef](#)]
68. Zou, C.; Klintberg, A.; Wei, Z.; Fridholm, B.; Wik, T.; Egardt, B. Power capability prediction for lithium-ion batteries using economic nonlinear model predictive control. *J. Power Sources* **2018**, *396*, 580–589. [[CrossRef](#)]
69. Karlsen, H.; Dong, T.; Yang, Z.; Carvalho, R. Temperature-Dependence in Battery Management Systems for Electric Vehicles: Challenges, Criteria, and Solutions. *IEEE Access* **2019**, *7*, 142203–142213. [[CrossRef](#)]
70. You, H.W.; Bae, J.I.; Cho, S.J.; Lee, J.M.; Kim, S.-H. Analysis of equivalent circuit models in lithium-ion batteries. *AIP Adv.* **2018**, *8*, 125101. [[CrossRef](#)]
71. How, D.; Hannan, M.; Lipu, M.S.H.; Ker, P.J. State of Charge Estimation for Lithium-Ion Batteries Using Model-Based and Data-Driven Methods: A Review. *IEEE Access* **2019**, *7*, 136116–136136. [[CrossRef](#)]
72. Hentunen, A.; Lehmuspelto, T.; Suomela, J. Time-Domain Parameter Extraction Method for Thévenin-Equivalent Circuit Battery Models. *IEEE Trans. Energy Convers.* **2014**, *29*, 558–566. [[CrossRef](#)]
73. Li, Y.; Abdel-Monem, M.; Gopalakrishnan, R.; Berecibar, M.; Maury, E.N.; Omar, N.; Bossche, P.; Mierlo, J.V. A quick on-line state of health estimation method for Li-ion battery with incremental capacity curves processed by Gaussian filter. *J. Power Sources* **2018**, *373*, 40–53. [[CrossRef](#)]
74. Wang, W.; Gaillard, A.; Hissel, D. Online electrochemical impedance spectroscopy detection integrated with step-up converter for fuel cell electric vehicle. *Int. J. Hydrogen Energy* **2019**, *44*, 1110–1121. [[CrossRef](#)]
75. Xing, J.; Wu, P. State of Charge Estimation of Lithium-Ion Battery Based on Improved Adaptive Unscented Kalman Filter. *Sustainability* **2021**, *13*, 5046. [[CrossRef](#)]
76. Morello, R.; Di Rienzo, R.; Roncella, R.; Saletti, R.; Baronti, F. Hardware-in-the-loop platform for assessing battery state estimators in electric vehicles. *IEEE Access* **2018**, *6*, 68210–68220. [[CrossRef](#)]
77. Wang, W.; Wang, X.; Xiang, C.; Wei, C.; Zhao, Y. Unscented Kalman filter-based battery SoC estimation and peak power prediction method for power distribution of hybrid electric vehicles. *IEEE Access* **2018**, *6*, 35957–35965. [[CrossRef](#)]
78. Lipu, M.S.H.; Hussain, A.; Saad, M.H.M.; Ayob, A.; Hannan, M.A. Improved Recurrent NARX Neural Network Model for State of Charge Estimation of Lithium-ion Battery Using PSO Algorithm. In Proceedings of the IEEE Symposium on Computer Applications & Industrial Electronics (ISCAIE), Penang, Malaysia, 28–29 April 2018; pp. 354–359.
79. Wu, X.; Li, X.; Du, J. State of charge estimation of lithium-ion batteries over wide temperature range using unscented Kalman filter. *IEEE Access* **2018**, *6*, 41993–42003. [[CrossRef](#)]
80. Xu, G.; Du, X.; Li, Z.; Zhang, X.; Zheng, M.; Miao, Y.; Gao, Y.; Liu, Q. Reliability design of battery management system for power battery. *Microelectron. Reliab.* **2018**, *88–90*, 1286–1292. [[CrossRef](#)]
81. Hu, X.; Zhang, K.; Liu, K.; Lin, X.; Dey, S.; Onori, S. Advanced Fault Diagnosis for Lithium-Ion Battery Systems: A Review of Fault Mechanisms, Fault Features, and Diagnosis Procedures. *IEEE Ind. Electron. Mag.* **2020**, *14*, 65–91. [[CrossRef](#)]
82. Momma, T.; Matsunaga, M.; Mukoyama, D.; Osaka, T. Ac impedance analysis of lithium ion battery under temperature control. *J. Power Sources* **2012**, *216*, 304–307. [[CrossRef](#)]
83. Marongiu, A.; Nußbaum, F.H.W.; Waag, W.; Garmendia, M.; Sauer, D.U. Comprehensive study of the influence of aging on the hysteresis behavior of a lithium iron phosphate cathode-based lithium ion battery—An experimental investigation of the hysteresis. *Appl. Energy* **2016**, *171*, 629–645. [[CrossRef](#)]
84. Han, X.; Ouyang, M.; Lu, L.; Li, J.; Zheng, Y.; Li, Z. A comparative study of commercial lithium ion battery cycle life in electrical vehicle: Aging mechanism identification. *J. Power Sources* **2014**, *251*, 38–54. [[CrossRef](#)]
85. Zheng, Y.; Ouyang, M.; Lu, L.; Li, J.; Han, X.; Xu, L.; Ma, H.; Dollmeyer, T.A.; Freyermuth, V. Cell state-of-charge inconsistency estimation for LiFePO<sub>4</sub> battery pack in hybrid electric vehicles using mean-difference model. *Appl. Energy* **2013**, *111*, 571–580. [[CrossRef](#)]
86. Ezemobi, E.; Tonoli, A.; Silvagni, M. Battery State of Health Estimation with Improved Generalization Using Parallel Layer Extreme Learning Machine. *Energies* **2021**, *14*, 2243. [[CrossRef](#)]
87. Lavigne, L.; Sabatier, J.; Francisco, J.M.; Guillemard, F.; Noury, A. Lithium-ion Open Circuit Voltage (OCV) curve modelling and its ageing adjustment. *J. Power Sources* **2016**, *324*, 694–703. [[CrossRef](#)]
88. Xing, Y.; He, W.; Pecht, M.; Tsui, K.L. State of charge estimation of lithium-ion batteries using the open-circuit voltage at various ambient temperatures. *Appl. Energy* **2014**, *113*, 106–115. [[CrossRef](#)]

89. Zhang, Y.; Song, W.; Lin, S.; Feng, Z. A novel model of the initial state of charge estimation for LiFePO<sub>4</sub> batteries. *J. Power Sources* **2014**, *248*, 1028–1033. [[CrossRef](#)]
90. Roscher, M.A.; Sauer, D.U. Dynamic electric behavior and open-circuit-voltage modeling of LiFePO<sub>4</sub>-based lithium ion secondary batteries. *J. Power Sources* **2011**, *196*, 331–336. [[CrossRef](#)]
91. Zhu, L.; Sun, Z.; Dai, H.; Wei, X. A novel modeling methodology of open circuit voltage hysteresis for LiFePO<sub>4</sub> batteries based on an adaptive discrete Preisach model. *Appl. Energy* **2015**, *155*, 91–109. [[CrossRef](#)]
92. Unterrieder, C.; Zhang, C.; Lunglmayr, M.; Priewasser, R.; Marsili, S.; Huemer, M. Battery state-of-charge estimation using approximate least squares. *J. Power Sources* **2015**, *278*, 274–286. [[CrossRef](#)]
93. Petzl, M.; Danzer, M.A. Advancements in OCV Measurement and Analysis for Lithium-Ion Batteries. *IEEE Trans. Energy Convers.* **2013**, *28*, 675–681. [[CrossRef](#)]
94. Pei, L.; Wang, T.; Lu, R.; Zhu, C. Development of a voltage relaxation model for rapid open-circuit voltage prediction in lithium-ion batteries. *J. Power Sources* **2014**, *253*, 412–418. [[CrossRef](#)]
95. Pei, L.; Lu, R.; Zhu, C. Relaxation model of the open-circuit voltage for state-of-charge estimation in lithium-ion batteries. *IET Electr. Syst. Transp.* **2013**, *3*, 112–117. [[CrossRef](#)]
96. Waag, W.; Sauer, D.U. Adaptive estimation of the electromotive force of the lithium-ion battery after current interruption for an accurate state-of-charge and capacity determination. *Appl. Energy* **2013**, *111*, 416–427. [[CrossRef](#)]
97. Hu, Y.; Yurkovich, S. Battery cell state-of-charge estimation using linear parameter varying system techniques. *J. Power Sources* **2012**, *198*, 338–350. [[CrossRef](#)]
98. Wenzl, H. Batteries and fuel cells; Efficiency. In *Encyclopedia of Electrochemical Power Sources*; Elsevier: Amsterdam, The Netherlands, 2009; pp. 544–551.
99. Truchot, C.; Dubarry, M.; Liaw, B.Y. State-of-charge estimation and uncertainty for lithium-ion battery strings. *Appl. Energy* **2014**, *119*, 2018–2227. [[CrossRef](#)]
100. Tang, X.; Wang, Y.; Chen, Z. A method for state-of-charge estimation of LiFePO<sub>4</sub> batteries based on a dual-circuit state observer. *J. Power Sources* **2015**, *296*, 23–29. [[CrossRef](#)]
101. Duong, V.-H.; Bastawrous, H.A.; Lim, K.; See, K.W.; Zhang, P.; Dou, S.X. Online state of charge and model parameters estimation of the LiFePO<sub>4</sub> battery in electric vehicles using multiple adaptive forgetting factors recursive least-squares. *J. Power Sources* **2015**, *296*, 215–224. [[CrossRef](#)]
102. Chiang, Y.-H.; Sean, W.-Y.; Ke, J.-C. Online estimation of internal resistance and open-circuit voltage of lithium-ion batteries in electric vehicles. *J. Power Sources* **2011**, *196*, 3921–3932. [[CrossRef](#)]
103. Dai, H.; Xu, T.; Zhu, L.; Wei, X.; Sun, Z. Adaptive model parameter identification for large capacity Li-ion batteries on separated time scales. *Appl. Energy* **2016**, *184*, 119–131. [[CrossRef](#)]
104. Wei, Z.; Meng, S.; Xiong, B.; Ji, D.; Tseng, K.J. Enhanced online model identification and state of charge estimation for lithium-ion battery with a FBCRLS based observer. *Appl. Energy* **2016**, *181*, 232–241. [[CrossRef](#)]
105. Fuyuan, S.; Zhenglin, L.; Long, X.; Jiang, F.; Hua, W. Research on Estimation of Battery State of Electric Vehicle Battery Management System. In Proceedings of the IEEE 5th Information Technology and Mechatronics Engineering Conference (ITOEC), Chongqing, China, 12–14 June 2020; pp. 465–469.
106. Sepasi, S.; Ghorbani, R.; Liaw, B.Y. Improved extended Kalman filter for state of charge estimation of battery pack. *J. Power Sources* **2014**, *255*, 368–376. [[CrossRef](#)]
107. Balasingam, B.; Avvari, G.V.; Pattipati, B.; Pattipati, K.R.; Bar-Shalom, Y. A robust approach to battery fuel gauging, part I: Real time model identification. *J. Power Sources* **2014**, *272*, 1142–1153. [[CrossRef](#)]
108. Ouyang, M.; Liu, G.; Lu, L.; Li, J.; Han, X. Enhancing the estimation accuracy in low state-of-charge area: A novel onboard battery model through surface state of charge determination. *J. Power Sources* **2014**, *270*, 221–237. [[CrossRef](#)]
109. He, H.; Xiong, R.; Peng, J. Real-time estimation of battery state-of-charge with unscented Kalman filter and RTOS  $\mu$ COS-II platform. *Appl. Energy* **2016**, *162*, 1410–1418. [[CrossRef](#)]
110. Yang, F.; Xing, Y.; Wang, D.; Tsui, K.-L. A comparative study of three model-based algorithms for estimating state-of-charge of lithium-ion batteries under a new combined dynamic loading profile. *Appl. Energy* **2016**, *164*, 387–399. [[CrossRef](#)]
111. Sun, F.; Xiong, R.; He, H.; Li, W.; Aussems, J.E.E. Model-based dynamic multi-parameter method for peak power estimation of lithium-ion batteries. *Appl. Energy* **2012**, *96*, 378–386. [[CrossRef](#)]
112. Verma, M.K.S.; Basu, S.; Patil, R.S.; Hariharan, K.S.; Adiga, S.P.; Kolake, S.M.; Oh, D.; Song, T.; Sung, Y. On-Board State Estimation in Electrical Vehicles: Achieving Accuracy and Computational Efficiency Through an Electrochemical Model. *IEEE Trans. Veh. Technol.* **2020**, *69*, 2563–2575. [[CrossRef](#)]
113. Li, J.; Lai, Q.; Wang, L.; Lyu, C.; Wang, H. A method for SOC estimation based on simplified mechanistic model for LiFePO<sub>4</sub> battery. *Energy* **2016**, *114*, 1266–1276. [[CrossRef](#)]
114. Li, J.; Wang, L.; Lyu, C.; Pecht, M. State of charge estimation based on a simplified electrochemical model for a single LiCoO<sub>2</sub> battery and battery pack. *Energy* **2017**, *133*, 572–583. [[CrossRef](#)]
115. Zhang, T.; Guo, N.; Sun, X.; Fan, J.; Yang, N.; Song, J.; Zou, Y. A Systematic Framework for State of Charge, State of Health and State of Power Co-Estimation of Lithium-Ion Battery in Electric Vehicles. *Sustainability* **2021**, *13*, 5166. [[CrossRef](#)]

116. Han, X.; Ouyang, M.; Lu, L.; Li, J. Simplification of physics-based electrochemical model for lithium ion battery on electric vehicle. Part II: Pseudo-two-dimensional model simplification and state of charge estimation. *J. Power Sources* **2015**, *278*, 814–825. [[CrossRef](#)]
117. Wang, Y.; Fang, H.; Sahinoglu, Z.; Wada, T.; Hara, S. Adaptive Estimation of the State of Charge for Lithium-Ion Batteries: Nonlinear Geometric Observer Approach. *IEEE Trans. Contr. Syst. Trans.* **2015**, *23*, 948–962. [[CrossRef](#)]
118. Crocioni, G.; Pau, D.; Delorme, J.-M.; Gruosso, G. Li-Ion Batteries Parameter Estimation with Tiny Neural Networks Embedded on Intelligent IoT Microcontrollers. *IEEE Access* **2020**, *8*, 122135–122146. [[CrossRef](#)]
119. Turksoy, A.; Teke, A.; Alkaya, A. A comprehensive overview of the dc-dc converter-based battery charge balancing methods in electric vehicles. *Renew. Sustain. Energy Rev.* **2020**, *133*, 1–20. [[CrossRef](#)]
120. Vidal, C.; Haußmann, M.; Barroso, D.; Shamsabadi, P.M.; Biswas, A.; Chemali, E.; Ahmed, R.; Emadi, A. Hybrid Energy Storage System State-of-Charge Estimation Using Artificial Neural Network for Micro-Hybrid Applications. In Proceedings of the IEEE Transportation Electrification Conference and Expo (ITEC), Long Beach, CA, USA, 13–15 June 2018; pp. 1075–1081.
121. Liu, H.; Gegov, A.; Cocea, M. *Rule Based Systems for Big Data*; Springer: Cham, Switzerland, 2016; Volume 13.
122. Chemali, E.; Kollmeyer, P.J.; Preindl, M.; Emadi, A. State-of-charge estimation of Li-ion batteries using deep neural networks: A machine learning approach. *J. Power Sour.* **2018**, *400*, 242–255. [[CrossRef](#)]
123. Hannan, M.A.; Lipu, M.S.H.; Hussain, A.; Mohamed, A. A review of lithium-ion battery state of charge estimation and management system in electric vehicle applications: Challenges and recommendations. *Renew. Sustain. Energy Rev.* **2017**, *78*, 834–854. [[CrossRef](#)]
124. Emadi, A. *Advanced Electric Drive Vehicles*; CRC Press: New York, NY, USA, 2015.
125. Hu, Y.; Wang, Z. Study on SOC Estimation of Lithium Battery Based on Improved BP Neural Network. In Proceedings of the 8th International Symposium on Next Generation Electronics (ISNE), Zhengzhou, China, 9–10 October 2019; pp. 1–3.
126. Hannan, M.A.; Lipu, M.S.H.; Hussain, A.; Saad, M.H.; Ayob, A. Neural Network Approach for Estimating State of Charge of Lithium-Ion Battery Using Backtracking Search Algorithm. *IEEE Access* **2018**, *6*, 10069–10079. [[CrossRef](#)]
127. Roscher, M.A.; Bohlen, O.S.; Sauer, D.U. Reliable State Estimation of Multicell Lithium-Ion Battery Systems. *IEEE Trans. Energy Conver.* **2011**, *26*, 737–743. [[CrossRef](#)]
128. Wang, S.; Verbrugge, M.; Wang, J.S.; Liu, P. Multi-parameter battery state estimator based on the adaptive and direct solution of the governing differential equations. *J. Power Sources* **2011**, *196*, 8735–8741. [[CrossRef](#)]
129. Nejad, S.; Gladwin, D.T. Online Battery State of Power Prediction Using PRBS and Extended Kalman Filter. *IEEE Trans. Ind. Electron.* **2020**, *67*, 3747–3755. [[CrossRef](#)]
130. Thenaisie, G.; Park, C.; Lee, S. A Real-Time Entropy Estimation Algorithm for Lithium Batteries Based on a Combination of Kalman Filter and Nonlinear Observer. *IEEE Trans. Ind. Electron.* **2020**, *67*, 8034–8043. [[CrossRef](#)]
131. Li, D.; Ouyang, J.; Li, H.; Wan, J. State of charge estimation for LiMn<sub>2</sub>O<sub>4</sub> power battery based on strong tracking sigma point Kalman filter. *J. Power Sources* **2015**, *279*, 439–449. [[CrossRef](#)]
132. Partovibakhsh, M.; Liu, G. An Adaptive Unscented Kalman Filtering Approach for Online Estimation of Model Parameters and State-of-Charge of Lithium-Ion Batteries for Autonomous Mobile Robots. *IEEE Trans. Contr. Syst.* **2015**, *23*, 357–363. [[CrossRef](#)]
133. Tian, Y.; Xia, B.; Sun, W.; Xu, Z.; Zheng, W. A modified model based state of charge estimation of power lithium-ion batteries using unscented Kalman filter. *J. Power Sources* **2014**, *270*, 619–626. [[CrossRef](#)]
134. Li, Y.; Wang, C.; Gong, J. A combination Kalman filter approach for State of Charge estimation of lithium-ion battery considering model uncertainty. *Energy* **2016**, *109*, 933–946. [[CrossRef](#)]
135. Zou, Y.; Hu, X.; Ma, H.; Li, S.E. Combined State of Charge and State of Health estimation over lithium-ion battery cell cycle lifespan for electric vehicles. *J. Power Sources* **2015**, *273*, 793–803. [[CrossRef](#)]
136. Sepasi, S.; Ghorbani, R.; Liaw, B.Y. A novel on-board state-of-charge estimation method for aged Li-ion batteries based on model adaptive extended Kalman filter. *J. Power Sources* **2014**, *245*, 337–344. [[CrossRef](#)]
137. Xiong, R.; Sun, F.; Chen, Z.; He, H. A data-driven multi-scale extended Kalman filtering based parameter and state estimation approach of lithium-ion polymer battery in electric vehicles. *Appl. Energy* **2014**, *113*, 463–476. [[CrossRef](#)]
138. Waag, W.; Käbitz, S.; Sauer, D.U. Experimental investigation of the lithium-ion battery impedance characteristic at various conditions and aging states and its influence on the application. *Appl. Energy* **2013**, *2*, 885–897. [[CrossRef](#)]
139. Eddahech, A.; Briat, O.; Woirgard, E.; Vinassa, J.M. Remaining useful life prediction of lithium batteries in calendar ageing for automotive applications. *Microelectron. Reliab.* **2012**, *52*, 2438–2442. [[CrossRef](#)]
140. Zhu, J.G.; Sun, Z.C.; Wei, X.Z.; Dai, H.F. A new lithium-ion battery internal temperature on-line estimate method based on electrochemical impedance spectroscopy measurement. *J. Power Sources* **2015**, *274*, 990–1004. [[CrossRef](#)]
141. Kim, I.-S. Nonlinear state of charge estimator for hybrid electric vehicle battery. *IEEE Trans. Power Electron.* **2008**, *23*, 2027–2034.
142. Zuboff, S. *The Age of Surveillance Capitalism: The Fight for a Human Future at the New Frontier of Power*, 1st ed.; PublicAffairs: New York, NY, USA, 2019.
143. Baumhöfer, T.; Brühl, M.; Rothgang, S.; Sauer, D.U. Production caused variation in capacity aging trend and correlation to initial cell performance. *J. Power Sources* **2014**, *247*, 332–338. [[CrossRef](#)]
144. Li, S.E.; Wang, B.; Peng, H.; Hu, X. An electrochemistry-based impedance model for lithium-ion batteries. *J. Power Sources* **2014**, *258*, 9–18. [[CrossRef](#)]

145. Plett, G.L. Extended Kalman filtering for battery management systems of LiPB-based HEV battery packs Part 1. Background. *J. Power Sources* **2004**, *134*, 252–261. [[CrossRef](#)]
146. Plett, G.L. Extended Kalman filtering for battery management systems of LiPB-based HEV battery packs: Part 2. Modeling and identification. *J. Power Sources* **2004**, *134*, 262–276. [[CrossRef](#)]
147. Plett, G.L. Extended Kalman filtering for battery management systems of LiPB-based HEV battery packs: Part 3. State and parameter estimation. *J. Power Sources* **2004**, *134*, 277–292. [[CrossRef](#)]
148. Xu, J.; Mi, C.C.; Cao, B.; Deng, J.; Chen, Z.; Li, S. The state of charge estimation of lithium-ion batteries based on a proportional-integral observer. *IEEE Trans. Veh. Technol.* **2014**, *63*, 1614–1621.
149. Zhang, F.; Liu, G.; Fang, L.; Wang, H. Estimation of battery state of charge with H1 observer: Applied to a robot for inspecting power transmission lines. *IEEE Trans. Ind. Electron.* **2012**, *59*, 1086–1095. [[CrossRef](#)]
150. Xiong, R.; Cao, J.; Yu, Q.; He, H.; Sun, F. Critical Review on the Battery State of Charge Estimation Methods for Electric Vehicles. *IEEE Access* **2019**, *6*, 1832–1843. [[CrossRef](#)]
151. Yatsui, M.W.; Bai, H. Kalman Filter Based State-of-Charge Estimation for Lithium-ion Batteries in Hybrid Electric Vehicles Using Pulse Charging. In Proceedings of the Vehicle Power and Propulsion Conference, Chicago, IL, USA, 6–9 September 2011; pp. 1–5.
152. Wei, J.; Dong, G.; Chen, Z. On-board adaptive model for state of charge estimation of lithium-ion batteries based on Kalman filter with proportional integral-based error adjustment. *J. Power Sources* **2017**, *365*, 308–319. [[CrossRef](#)]
153. He, H.; Liu, Z.; Hua, Y. Adaptive extended Kalman filter based fault detection and isolation for a lithium-ion battery pack. *Energy Procedia* **2015**, *75*, 1950–1955. [[CrossRef](#)]
154. Xia, B.; Sun, Z.; Zhang, R.; Lao, Z. A Cubature Particle Filter Algorithm to Estimate the State of the Charge of Lithium-Ion Batteries Based on a Second-Order Equivalent Circuit Model. *Energies* **2017**, *10*, 457. [[CrossRef](#)]
155. Ye, M.; Guo, H.; Xiong, R.; Yu, Q. A double-scale and adaptive particle filter-based online parameter and state of charge estimation method for lithium-ion batteries. *Energy* **2018**, *144*, 789–799. [[CrossRef](#)]
156. Ting, T.O.; Man, K.L.; Lim, E.G.; Leach, M. Tuning of Kalman Filter Parameters via Genetic Algorithm for State-of-Charge Estimation in Battery Management System. *Sci. World J.* **2014**, *2014*, 176052. [[CrossRef](#)] [[PubMed](#)]
157. Zhang, R.; Cao, L.; Bao, S.; Tan, J. A method for connected vehicle trajectory prediction and collision warning algorithm based on V2V communication. *Int. J. Crashworth.* **2017**, *22*, 15–25. [[CrossRef](#)]
158. Oyarbide, M.; Arrinda, M.; Sánchez, D.; Macicior, H.; McGahan, P.; Hoedemaekers, E.; Cendoya, I. Capacity and Impedance Estimation by Analysing and Modeling in Real Time Incremental Capacity Curves. *Energies* **2020**, *13*, 4855. [[CrossRef](#)]
159. Xiong, B.; Zhao, J.; Wei, Z.; Skyllas-Kazacos, M. Extended Kalman filter method for state of charge estimation of vanadium redox flow battery using thermal-dependent electrical model. *J. Power Sources* **2014**, *262*, 50–61. [[CrossRef](#)]
160. Xiong, R.; Gong, X.; Mi, C.C.; Sun, F. A robust state-of-charge estimator for multiple types of lithium-ion batteries using adaptive extended Kalman filter. *J. Power Sources* **2013**, *243*, 805–816. [[CrossRef](#)]
161. Xiong, R.; He, H.; Sun, F.; Zhao, K. Evaluation on State of Charge Estimation of Batteries with Adaptive Extended Kalman Filter by Experiment Approach. *IEEE Trans. Veh. Technol.* **2013**, *62*, 108–117. [[CrossRef](#)]
162. Zheng, F.; Xing, Y.; Jiang, J.; Sun, B.; Kim, J.; Pecht, M. Influence of different open circuit voltage tests on state of charge online estimation for lithium-ion batteries. *Appl. Energy* **2016**, *182*, 513–525. [[CrossRef](#)]
163. Plett, G.L. Sigma-point Kalman filtering for battery management systems of LiPB-based HEV battery packs: Part 1: Introduction and state estimation. *J. Power Sources* **2006**, *161*, 1356–1368. [[CrossRef](#)]
164. Plett, G.L. Sigma-point Kalman filtering for battery management systems of LiPB-based HEV battery packs: Part 2: Simultaneous state and parameter estimation. *J. Power Sources* **2006**, *161*, 1369–1384. [[CrossRef](#)]
165. He, Z.; Liu, Y.; Gao, M.; Wang, C. A Joint Model and SOC Estimation Method for Lithium Battery Based on the Sigma Point KF. In Proceedings of the Transportation Electrification Conference and Expo (ITEC), Dearborn, MI, USA, 18–20 June 2012; pp. 1–5.
166. Goodfellow, I.; Bengio, Y.; Courville, A. *Deep Learning*; MIT Press: Cambridge, MA, USA, 2016.
167. Xia, B.; Cui, D.; Sun, Z.; Lao, Z.; Zhang, R.; Wang, W.; Sun, W.; Lai, Y.; Wang, M. State of charge estimation of lithium-ion batteries using optimized Levenberg-Marquardt wavelet neural network. *Energy* **2018**, *153*, 694–705. [[CrossRef](#)]
168. Dang, X.; Yan, L.; Xu, K.; Wu, X.; Jiang, H.; Sun, H. Open-Circuit Voltage-Based State of Charge Estimation of Lithium-ion Battery Using Dual Neural Network Fusion Battery Model. *Electrochim. Acta* **2016**, *188*, 356–366. [[CrossRef](#)]
169. Tong, S.; Lacap, J.H.; Park, J.W. Battery state of charge estimation using a load-classifying neural network. *J. Energy Storage* **2016**, *7*, 236–243. [[CrossRef](#)]
170. Chaoui, H.; Ibe-Ekeocha, C.C.; Gualous, H. Aging prediction and state of charge estimation of a LiFePO<sub>4</sub> battery using input time-delayed neural networks. *Electr. Power Syst. Res.* **2017**, *146*, 189–197. [[CrossRef](#)]
171. Hu, J.N.; Hu, J.J.; Lin, H.B.; Li, X.P.; Jiang, C.L.; Qiu, X.H.; Li, W.S. State-of-charge estimation for battery management system using optimized support vector machine for regression. *J. Power Sources* **2014**, *269*, 682–693. [[CrossRef](#)]
172. Sheng, H.; Xiao, J. Electric vehicle state of charge estimation: Nonlinear correlation and fuzzy support vector machine. *J. Power Sources* **2015**, *281*, 131–137. [[CrossRef](#)]
173. Blaifi, S.; Moulahoum, S.; Colak, I.; Merrouche, W. An enhanced dynamic model of battery using genetic algorithm suitable for photovoltaic applications. *Appl. Energy* **2016**, *169*, 888–898. [[CrossRef](#)]
174. Xu, J.; Cao, B.; Chen, Z.; Zou, Z. An online state of charge estimation method with reduced prior battery testing information. *Int. J. Electr. Power Energy Syst.* **2014**, *63*, 178–184. [[CrossRef](#)]

175. Gao, Z.; Cing, C.S.; Woo, W.L.; Jia, J.; Toh, W.D. Genetic Algorithm Based Back-Propagation Neural Network Approach for Fault Diagnosis in Lithium-ion Battery System. In Proceedings of the International Conference on Power Electronics Systems and Applications (PESA), Hong Kong, China, 15–17 December 2015; pp. 1–6.
176. Awadallah, M.A.; Venkatesh, B. Accuracy improvement of SOC estimation in lithium-ion batteries. *J. Energy Storage* **2016**, *6*, 95–104. [CrossRef]
177. Dai, H.; Guo, P.; Wei, X.; Sun, Z.; Wang, J. ANFIS (Adaptive Neuro-Fuzzy Inference System) based online SOC (State of Charge) correction considering cell divergence for the EV (Electric Vehicle) traction batteries. *Energy* **2015**, *80*, 350–360. [CrossRef]
178. Wang, Q.-K.; He, Y.-J.; Shen, J.-N.; Hu, X.; Ma, Z.-F. State of Charge Dependent Polynomial Equivalent Circuit Modeling for Electrochemical Impedance Spectroscopy of Lithium-Ion Batteries. *IEEE Trans. Power Electron.* **2018**, *33*, 8449–8460. [CrossRef]
179. Yu, Z.; Xiao, L.; Li, H.; Zhu, X.; Huai, R. Model Parameter Identification for Lithium Batteries Using the Coevolutionary Particle Swarm Optimization Method. *IEEE Trans. Ind. Electron.* **2017**, *64*, 5690–5700. [CrossRef]
180. Wang, Z.; Ma, J.; Zhang, L. State-of-Health Estimation for Lithium-Ion Batteries Based on the Multi-Island Genetic Algorithm and the Gaussian Process Regression. *IEEE Access* **2017**, *5*, 21286–21295. [CrossRef]
181. Rahimi-Eichi, H.; Baronti, F.; Chow, M.-Y. Online Adaptive Parameter Identification and State-of-Charge Coestimation for Lithium-Polymer Battery Cells. *IEEE Trans. Ind. Electron.* **2014**, *61*, 2053–2061. [CrossRef]
182. Fan, G.; Li, X.; Canova, M. A Reduced-Order Electrochemical Model of Li-Ion Batteries for Control and Estimation Applications. *IEEE Trans. Veh. Technol.* **2018**, *67*, 76–91. [CrossRef]
183. Li, Y.; Liu, K.; Foley, A.M.; Zülke, A.; Berecibar, M.; Nanini-Maury, E.; Mierlo, J.V.; Hoster, H.E. Data-driven health estimation and lifetime prediction of lithium-ion batteries: A review. *Renew. Sustain. Energy Rev.* **2019**, *113*, 109254. [CrossRef]
184. Tan, X.; Tan, Y.; Zhan, D.; Yu, Z.; Fan, Y.; Qiu, J.; Li, J. Real-Time State-of-Health Estimation of Lithium-Ion Batteries Based on the Equivalent Internal Resistance. *IEEE Access* **2020**, *8*, 56811–56822. [CrossRef]
185. Stroe, D.; Schaltz, E. Lithium-Ion Battery State-of-Health Estimation Using the Incremental Capacity Analysis Technique. *IEEE Trans. Ind. Appl.* **2020**, *56*, 678–685. [CrossRef]
186. Sarrafan, K.; Muttaqi, K.; Sutanto, D. Real-time estimation of model parameters and state-of-charge of lithium-ion batteries in electric vehicles using recursive least-square with forgetting factor. In Proceedings of the IEEE International Conference on Power Electronics, Drives and Energy Systems (PEDES), Chennai, China, 18–21 December 2018; pp. 1–6.
187. Kim, J.; Cho, B.H. State-of-Charge Estimation and State-of-Health Prediction of a Li-Ion Degraded Battery Based on an EKF Combined with a Per-Unit System. *IEEE Trans. Veh. Technol.* **2011**, *60*, 4249–4260. [CrossRef]
188. Kim, I. A Technique for Estimating the State of Health of Lithium Batteries Through a Dual-Sliding-Mode Observer. *IEEE Trans. Power Electron.* **2010**, *25*, 1013–1022.
189. Kim, K.; Lee, S.; Cho, B. Discrimination of Battery Characteristics Using Discharging/Charging Voltage Pattern Recognition. In Proceedings of the IEEE Energy Conversion Congress and Exposition, San Jose, CA, USA, 24–27 September 2009; pp. 1799–1805.
190. Lievre, A.; Sari, A.; Venet, P.; Hijazi, A.; Ouattara-Brigaudet, M.; Pelissier, S. Practical Online Estimation of Lithium-Ion Battery Apparent Series Resistance for Mild Hybrid Vehicles. *IEEE Trans. Veh. Technol.* **2016**, *65*, 4505–4511. [CrossRef]
191. Zhao, S.; Wu, F.; Yang, L.; Gao, L.; Burke, A.F. A measurement method for determination of dc internal resistance of batteries and supercapacitors. *Electrochem. Commun.* **2010**, *12*, 242–245. [CrossRef]
192. Zenati, A.; Desprez, P.; Razik, H.; Rael, S. A Methodology to Assess the State of Health of Lithium-ion Batteries Based on the Battery's Parameters and a Fuzzy Logic System. In Proceedings of the IEEE International Electric Vehicle Conference, Greenville, SC, USA, 4–8 March 2012; pp. 1–6.
193. Chen, Y.; Liu, X.; Yang, G. An Internal Resistance Estimation Method of Lithium-ion Batteries with Constant Current Tests Considering Thermal Effect. In Proceedings of the 43rd Annual Conference of the IEEE Industrial Electronics Society (IECON), Beijing, China, 29 October–1 November 2017; pp. 7629–7635.
194. Gou, B.; Xu, Y.; Feng, X. State-of-Health Estimation and Remaining-Useful-Life Prediction for Lithium-Ion Battery Using a Hybrid Data-Driven Method. *IEEE Trans. Veh. Technol.* **2020**, *69*, 10854–10867. [CrossRef]
195. Islam, S.; Park, S. Precise Online Electrochemical Impedance Spectroscopy Strategies for Li-Ion Batteries. *IEEE Trans. Ind. Appl.* **2020**, *56*, 1161–1169. [CrossRef]
196. Legrand, N.; Raël, S.; Knosp, B.; Hinaje, M.; Desprez, P.; Lopicque, F. Including double-layer capacitance in lithium-ion battery mathematical models. *J. Power Sources* **2014**, *251*, 370–378. [CrossRef]
197. Gamry Instruments. Introduction to Electrochemical Impedance Spectroscopy. 2015. Available online: <https://www.gamry.com/assets/Uploads/Basics-of-Electrochemical-Impedance-Spectroscopy.pdf> (accessed on 31 May 2021).
198. Hossain, M.K.; Islam, S.M.R.; Park, S. Performance analysis of filter sensing board for measuring the battery online impedance. In Proceedings of the Asian Conference Energy, Power and Transportation Electrification (ACEPT), Singapore, 25–27 October 2016; pp. 1–6.
199. Kurzweil, P.; Scheuerpflug, W. State-of-Charge Monitoring and Battery Diagnosis of Different Lithium Ion Chemistries Using Impedance Spectroscopy. *Batteries* **2021**, *7*, 17. [CrossRef]
200. Qahouq, J.A.A. Online Battery Impedance Spectrum Measurement Method. In Proceedings of the IEEE Applied Power Electronics Conference and Exposition (APEC), Long Beach, CA, USA, 20–24 March 2016; pp. 3611–3615.
201. Din, E.; Schaefer, C.; Moffat, K.; Stauth, J.T. A Scalable Active Battery Management System with Embedded Real-Time Electrochemical Impedance Spectroscopy. *IEEE Trans. Power Electron.* **2017**, *32*, 5688–5698. [CrossRef]

202. Xia, Z.; Qahouq, J.A.A. An Online Battery Impedance Spectrum Measurement Method with Increased Frequency Resolution. In Proceedings of the IEEE Applied Power Electronics Conference and Exposition (APEC), San Antonio, TX, USA, 4–8 March 2018; pp. 1930–1933.
203. Li, W.; Huang, Q.; Yang, C.; Chen, J.; Tang, Z.; Zhang, F.; Li, A.; Zhang, L.; Zhang, J. A fast measurement of Warburg-like impedance spectra with Morlet wavelet transform for electrochemical energy devices. *Electrochim. Acta* **2019**, *322*, 134760. [[CrossRef](#)]
204. Okazaki, S.; Higuchi, S.; Kubota, N.; Takahashi, S. Predicted and observed initial short circuit current for lead-acid batteries. *J. Appl. Electrochem.* **1986**, *16*, 631–635. [[CrossRef](#)]
205. Mao, L.; Jackson, L.; Davies, B. Effectiveness of a Novel Sensor Selection Algorithm in PEM Fuel Cell On-Line Diagnosis. *IEEE Trans. Ind. Electron.* **2018**, *65*, 7301–7311. [[CrossRef](#)]
206. Yang, R.; Xiong, R.; He, H.; Chen, Z. A fractional-order model-based battery external short circuit fault diagnosis approach for all-climate electric vehicles application. *J. Cleaner Prod.* **2018**, *187*, 950–959. [[CrossRef](#)]
207. Chen, Z.; Xiong, R.; Lu, J.; Li, X. Temperature rise prediction of lithium-ion battery suffering external short circuit for all-climate electric vehicles application. *Appl. Energy* **2016**, *213*, 375–383. [[CrossRef](#)]
208. Spotnitz, R.; Franklin, J. Abuse behavior of high-power, lithium-ion cells. *J. Power Sources* **2003**, *113*, 81–100. [[CrossRef](#)]
209. Zhang, D.; Dey, S.; Perez, H.E.; Moura, S.J. Real-Time Capacity Estimation of Lithium-Ion Batteries Utilizing Thermal Dynamics. *IEEE Trans. Control. Syst. Technol.* **2020**, *28*, 992–1000. [[CrossRef](#)]
210. Hunt, I.A.; Patel, Y.; Szczygielski, M.; Kabacik, L.; Offer, G.J. Lithium sulfur battery nail penetration test under load. *J. Energy Storage* **2015**, *2*, 25–29. [[CrossRef](#)]
211. Leising, R.A.; Palazzo, M.J.; Takeuchi, E.S.; Takeuchi, K.J. Abuse Testing of Lithium-Ion Batteries: Characterization of the Overcharge Reaction of LiCoO<sub>2</sub>/Graphite Cells. *J. Electrochem. Soc.* **2001**, *148*, 838–844. [[CrossRef](#)]
212. Mevawalla, A.; Panchal, S.; Tran, M.-K.; Fowler, M.; Fraser, R. Mathematical Heat Transfer Modeling and Experimental Validation of Lithium-Ion Battery Considering: Tab and Surface Temperature, Separator, Electrolyte Resistance, Anode-Cathode Irreversible and Reversible Heat. *Batteries* **2020**, *6*, 61. [[CrossRef](#)]
213. El Mejdoubi, A.; Oukaour, A.; Chaoui, H.; Gualous, H.; Sabor, J.; Slamani, Y. State-of-Charge and State-of-Health Lithium-Ion Batteries' Diagnosis According to Surface Temperature Variation. *IEEE Trans. Ind. Electron.* **2016**, *63*, 2391–2402. [[CrossRef](#)]
214. Wang, Y.; Chen, Z.; Zhang, C. On-line remaining energy prediction: A case study in embedded battery management system. *Appl. Energy* **2017**, *194*, 688–695. [[CrossRef](#)]
215. Wang, Q.-K.; He, Y.-J.; Shen, J.-N.; Ma, Z.-F.; Zhong, G.-B. A unified modeling framework for lithium-ion batteries: An artificial neural network based thermal coupled equivalent circuit model approach. *Energy* **2017**, *138*, 118–132. [[CrossRef](#)]
216. Altaf, F.; Egardt, B.; Mårdh, L.J. Load Management of Modular Battery Using Model Predictive Control: Thermal and State-of-Charge Balancing. *IEEE Trans. Control Syst. Technol.* **2017**, *25*, 47–62. [[CrossRef](#)]
217. Farag, M.; Sweity, H.; Fleckenstein, M.; Habibi, S. Combined electrochemical, heat generation, and thermal model for large prismatic lithium-ion batteries in real-time applications. *J. Power Sources* **2017**, *360*, 618–633. [[CrossRef](#)]
218. You, G.-W.; Park, S.; Oh, D. Real-time state-of-health estimation for electric vehicle batteries: A data-driven approach. *Appl. Energy* **2016**, *176*, 92–103. [[CrossRef](#)]
219. Chemali, E.; Kollmeyer, P.J.; Preindl, M.; Ahmed, R.; Emadi, A. Long Short-Term Memory Networks for Accurate State-of-Charge Estimation of Li-ion Batteries. *IEEE Trans. Ind. Electron.* **2018**, *65*, 6730–6739. [[CrossRef](#)]
220. Salaken, S.M.; Khosravi, A.; Nguyen, T.; Nahavandi, S. Seeded transfer learning for regression problems with deep learning. *Expert Syst. Appl.* **2019**, *115*, 565–577. [[CrossRef](#)]
221. He, Y.; Tian, Y.; Liu, D. Multi-view transfer learning with privileged learning framework. *Neurocomputing* **2019**, *335*, 131–142. [[CrossRef](#)]